GATE VOLTAGE DEPENDENCE OF LOW FREQUENCY NOISE OF AlGaN/GaN HEMTs

By

Pan Wang

Thesis

Submitted to the Faculty of the

Graduate School of Vanderbilt University

in partial fulfillment of the requirements

for the degree of

MASTER OF SCIENCE

in

Electrical Engineering

May, 2017

Nashville, Tennessee

Approved:

Professor Daniel Fleetwood

Professor En Xia Zhang

ACKNOWLEDGEMENTS

First and foremost, I would like to express my sincere gratitude to my advisor, Dr. Daniel Fleetwood for his professional guidance and encouragement. His ideas and tremendous support had a major influence on this thesis. I am continually amazed by his broad and profound knowledge in microelectronics and radiation effects area. His approach to educating young scholars also inspires me a lot. I have been extremely lucky to have Dr. Fleetwood as my advisor.

I feel thankful to Dr. Ronald Schrimpf for teaching me the device physics and all the helpful discussion and insightful suggestions at the group meeting. I would also like to thank Dr. Robert Reed for providing lots of new insight into my work.

Many other people contribute to this work. Special thank you goes to Dr. Enxia Zhang. She is so patient, warmhearted and always there to help. I am extremely grateful for her assistance and suggestions though this project.

I would also like to thank my fellow graduate students in the Radiation Effects and Reliability group for offering me lots of help not only in the research work but also in my life.

I thank DTRA, and AFOSR and AFRL through the Hi-REV program for supporting this project. I would also like to acknowledge Dr. Anthony Hmelo and Mike McCurdy for their experimental support.

At last, I would like to thank my parents for their unconditional love and support. I heartily appreciate my family for their never ending encouragement and I thank my boyfriend, Wei Xie, for making my life colorful.

TABLE OF CONTENTS

LIST OF FIGURES

Figure **Page**

LIST OF TABLES

ABSTRACT

Low frequency noise measurements have been widely used to investigate the nature of defects in semiconductor devices. Characterization of low frequency noise performance at different gate bias along with the temperature is very useful to study and identify the defects in the devices.

In this work, the frequency, gate bias and temperature dependence of low frequency noise of three differently processed AlGaN/GaN high electron mobility transistors (HEMTs) have been evaluated. Both the frequency-dependence and gate-voltage dependence of the low frequency noise of AlGaN/GaN HEMTs are difficult to understand within the context of the popular Hooge mobility fluctuation model. Instead, the noise is consistent with a carrier-number fluctuation model that includes a non-constant defect-energy distribution $D_t(E_f)$. A strongly varying $D_t(E_f)$ in these devices is confirmed by measurements of the temperature dependence of the noise. Estimates of the effective border-trap density before and after 1.8 MeV proton irradiation are provided for both commercial and research-grade devices using a number-fluctuation model. The input-referred noise magnitude for AlGaN/GaN HEMTs decreases at biases that are significantly more positive than the threshold voltage because the gated region of the HEMT comprises a relatively small portion of the channel, and the noise is attenuated by the voltage divider formed by the gated and ungated regions of the channel.

CHAPTER I

INTRODUCTION

Overview of GaN HEMTs

Silicon technology has dominated the semiconductor industry for several decades. However, in areas like laser diodes, radio frequency and microwave power amplifiers, wide bandgap semiconductor materials like SiC and GaN can overtake the limit of silicon due to their material properties. As one of the most promising devices, Aluminum Gallium Nitride/Gallium Nitride (AlGaN/GaN) high electron mobility transistors (HEMTs) have gained increasing popularity in high power and high frequency applications, ever since the first AlGaN/GaN HEMT was introduced in 1993 [1]. The desirable properties of GaN such as the wide bandgap (3.4 eV), high saturated electron velocity (~2.5×10^7 cm/s), and high breakdown field (~3.1 MV/cm) enable the material tremendous potential. Table 1.1 shows the comparison of the key electronic properties of GaN with other materials [2].

Most importantly, GaN based HEMTs could take advantage of the high two dimensional electron gas (2DEG) sheet density. The 2DEG is formed when the conduction band of the barrier layer is higher than the conduction band of the channel layer. In contrast to other conventional III-V HEMTs like GaAs- and InP- based HEMTs, which require n-type doping to form high electron density sheets, spontaneous piezoelectric polarization contributes to a large interface sheet charge in GaN based HEMTs. Both AlGaN and GaN have strong spontaneous polarization, with larger polarization in AlGaN than that in GaN [3]. What's more, due to the mismatch of lattice constants of AlGaN and GaN, AlGaN layers grown on the GaN experience mechanical

strain, which leads to additional polarization at the interface, piezoelectric polarization [4]. The combination of large conduction and valence band discontinuities induced spontaneous polarization and the piezoelectric polarization leads to the extremely high sheet carrier densities in the channel of GaN devices ($> 10^{13}$ cm^{-2}) without intentional doping [4].

Table 1.1 the material properties of GaN compared to other competing materials (after [2]).

	Si	GaAs	InP	SiC	GaN
E_G (eV)	1.1	1.42	1.35	3.26	3.40
μ ($cm^2/V{\cdot}s$)	1500	8500	5400	700	1000-2000
v_{sat} (10^7 cm/s)	1	1.3	1	2	2.5
E_{br} ($\times 10^6$ V/cm)	0.3	0.4	0.5	3	3.3
κ (W/cm·K)	1.5	0.5	0.7	4.5	>1.5
ε_r (static)	11.8	12.8	12.5	10	9

A typical structure of AlGaN/GaN HEMTs is shown in Fig. 1-1. The drain and source terminals are both ohmic contacts and control the carriers in the direction parallel to the heterointerface. The gate terminal is a Schottky barrier contact, which controls the potential distribution of heterostructure below the contact bias [2]. The magnitude of current between the source and drain is controlled by the space charge, which is changed by applying the voltage to gate contact.

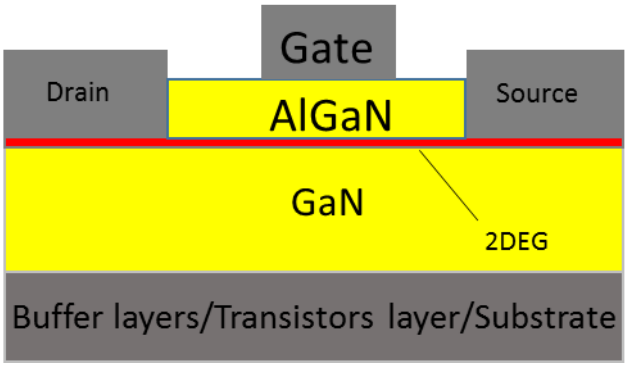

Fig. 1-1 Typical structure of AlGaN/GaN HEMTs. The 2DEG is formed inside the GaN layer, very near to the interface.

Radiation Effects and Low Frequency Noise

When energetic particles travel through semiconductor devices, the energy is lost due to ionizing and nonionizing processes. The energy loss causes the production of electron-hole pairs (ionization) and displaced atoms (displacement damage). Due to the high surface state density in GaN and usually absence of oxide layer, GaN based HEMTs are typically more tolerant to ionizing radiation [5], [6] than Si based MOSFETs. Therefore, a bigger concern than ionizing effects for GaN HEMTs is displacement damage.

After irradiation exposure, GaN HEMTs typically exhibit a shift in threshold voltage, increase in junction leakage and mobility degradation. Additionally, the low frequency noise generally increases [8]-[11].

In MOS devices, the low frequency noise magnitude of unirradiated MOS transistors is found to correlate with the radiation induced hole trapping efficiency of the oxide, which suggests that the defect responsible for $1/f$ noise is linked to the E' center, or a direct precursor [12]. People also found that $1/f$ noise has a strong correlation with oxide trapped charge, but not

interface trap charge [13], [14], as shown in Figs. 1-2. These findings lead to the conclusions that oxide traps within a few nm of the Si-SiO_2 interface, defined as border traps, are responsible for 1/*f* noise in MOS devices [15].

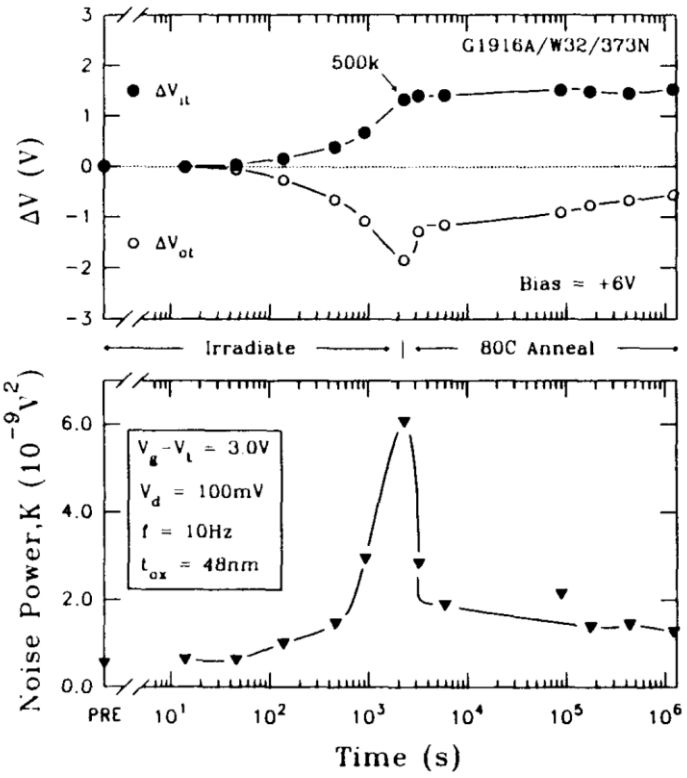

Fig. 1-2 Top: threshold voltage shifts due to interface trap charge (ΔV_{it}) and oxide trap charge (ΔV_{ot}) as functions of irradiation and annealing time for 3 μm long, 16 μm wide n-channel MOS transistors with ~ 50 nm oxides. Bottom: normalized noise power through the same irradiation and annealing. (After [14])

Similar to MOS devices, it is possible to approximately estimate the border trap density in GaN HEMTs using low frequency noise measurement. Additionally, since low frequency noise is quite sensitive to traps and defects and strongly related to physical processes like trapping/detrapping and release phenomena, low frequency noise measurements have been

applied as a diagnostic tool for radiation effects an help to locate and identify the defects in GaN HEMTs [8]-[11].

Previous work involving studies of the 1/*f* noise of GaN HEMTs as a function of temperature (Fig. 1-3) has revealed significant insight into the nature and microstructure of the defects [8]-[11]. In Fig. 1-3, before irradiation, there are two peaks observed with activation energies of about 0.2 eV and 0.7 eV. After irradiation, the noise magnitude of low temperature peak and ~300 K peak increase. Then DFT calculations were performed to identify the defects responsible for peaks in the energy distributions and found that the 0.2 eV peak is most likely due to an to N vacancy-related defects in GaN and O_N defects in AlGaN and the ~ 0.7 eV trap level in GaN is associated with a N_{Ga} defect, with their atomic structures shown in Fig. 1-4 [11].

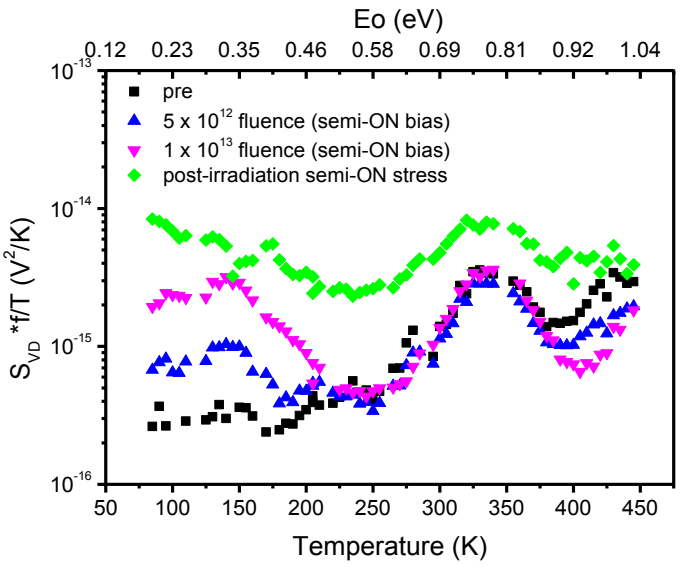

Fig. 1-3 Temperature-dependent noise measurements from 85 K to 445 K, for semi-ON state irradiation. (After [11])

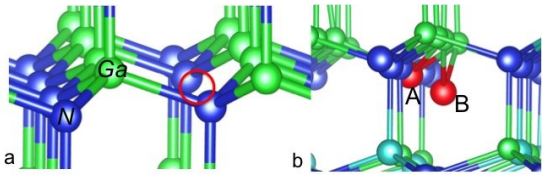

(a)

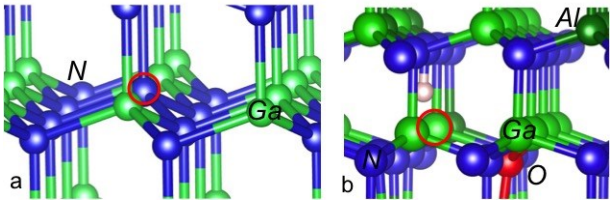

(b)

Fig. 1-4 (a) Atomic structure of the defects related to the ~ 0.2 eV noise peak, and (b) atomic structure of the defects potentially related to the previously unidentified ~ 0.7 eV peak in GaN. (after [11])

Motivation and Overview of Thesis

Compelling evidence from a number of studies demonstrates that the low-frequency noise of Si-based MOS devices is dominated by number fluctuations [16]-[18]. However, the Hooge mobility fluctuation model is still commonly used to analyze, parameterize, and/or explain the gate-voltage and/or channel-current dependence of low-frequency noise in AlGaN/GaN HEMTs [8], [19]-[24].

In this thesis, we present new results on the gate-voltage dependence of the low-frequency noise of AlGaN/GaN HEMTs built in three process technologies; two are commercial (Qorvo, Cree) processes, and one is a state-of-the-art development stage process (University of California at Santa Barbara, UCSB). The low frequency noise of AlGaN/GaN HEMTs are evaluated as a function of gate bias, proton fluence and temperature. We compare results with expectations

based on the Hooge's mobility fluctuation model and a number fluctuation model. Measurements and analysis of the voltage- and current-dependence of the noise, as well as the temperature dependence of the noise, show that the noise is more consistent with a number fluctuation model with a non-constant $D_t(E)$, similar to the case for Si-based MOSFETs.

Chapter II provides background of low frequency noise and reviews the two popular models of low frequency noise in semiconductor devices. The noise model of gate voltage dependence of 1/*f* noise of AlGaN/GaN HEMTs is also introduced.

The structure and measurement techniques employed in this work are shown in Chapter III. All the DC characteristics and low frequency noise measurement later are using the same experimental settings.

The low frequency noise is performed before and after proton irradiation in Chapter IV. Both the frequency dependence and gate voltage dependence consistent with the carrier-number fluctuation model that includes a non-constant defect-energy distribution $D_t(E_f)$.

In Chapter V, the temperature dependence of low frequency noise is shown and a strongly varying $D_t(E_f)$ in these devices is confirmed.

Chapter VI provides the summary and conclusions of this work.

CHAPTER II

LOW FREQUENCY NOISE THEORY

In this chapter, the background of low frequency noise is provided. Two widely used low frequency noise models are evaluated: the number fluctuation model and the Hooge's mobility fluctuation model.

Introduction of 1/f Noise

When current passes through a resistor, it is often found that, in addition to the thermal noise and shot noise, there is another excess noise in the low frequency range. The noise magnitude typically is found to be proportional to $1/f^{\alpha}$ (with α in the range 0.8~1.4) and frequently called low frequency noise, $1/f$ noise, flicker noise or pink noise. Fig. 2-1 is a typical low frequency noise spectrum of AlGaN/GaN HEMTs, showing the drain voltage noise power spectral density (S_{vd}) versus frequency. Low frequency noise exists in all semiconductor devices under biasing conditions and increases when the dimension of devices decreases, which could be a real problem for devices fabricated in nanoscale. The level of $1/f$ noise is a very useful parameter to evaluate the quality and reliability of devices.

Extensive experimental and theoretical work has been done to understand the mechanism that causes the low frequency noise in semiconductor devices. Although physical mechanisms and models of low frequency noise continue to be proposed, a clear conclusion has never been reached so far. Among all these models, McWhorter's number fluctuation model and Hooge's mobility fluctuation model are the most popular ones.

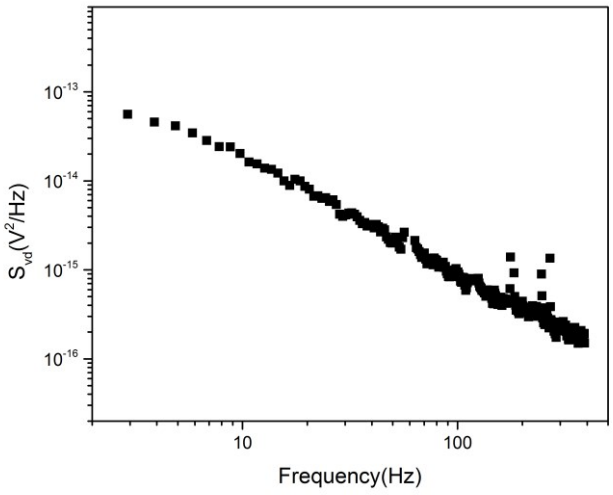

Fig. 2-1 Noise example: drain voltage noise power spectral density as a function of frequency.

The origin of low frequency noise is caused by the fluctuations in the conductivity σ,

$$\sigma = q(\mu_n n + \mu_p p) \tag{1}$$

Here q is the electronic charge, μ_n and μ_p are electron mobility and hole mobility respectively, n and p are electron and hole density, respectively. From Eq. (1), it is clear that the fluctuations in the conductivity could result either from the fluctuations in the carrier number or variations of the mobility or both. Thus two schools of thoughts regarding the origin of low frequency noise appear: number fluctuation model and mobility fluctuation model. According to the McWhorter model [25], charge carriers tunneling forth and back between the bulk and the defects lead to the fluctuations in the trap occupancy, thus causing the $1/f$ noise, while Hooge's mobility model suggests the low frequency noise is a bulk effect rather than a surface effect [26].

In the following parts of Chapter II, both of these two models and the device noise model will be reviewed to give foundational understanding of this thesis.

Number Fluctuation Model

Carrier number fluctuation model is also called trapping and detrapping model, proposed by McWhorther in 1957 [25], in which low frequency noise was attributed by the carrier number fluctuations in the channel. The physical mechanism behind the number fluctuation noise is the interaction between the traps in the channel. The traps exchange carriers with the channel causing a fluctuation in the surface potential, giving rise to fluctuations in the inversion charge density, which in turn causes the noise in the drain current.

a. Generation and Recombination Noise

In semiconductor devices and materials, generation-recombination (g-r) noise is due to the fluctuations in the number of free carriers associated with random transitions of charge carriers between states in different energy bands [27].

As a simple model, assuming the generation and recombination rate to be g(N) and r(N) respectively, it is possible to model the g-r noise from the fluctuations in the number of carriers by:

$$\frac{dN}{dt} = g(N) - r(N) + \Delta g(t) - \Delta r(t) \tag{2}$$

and get the expression of g-r noise [28]:

$$S_N(f) = \overline{4\Delta N^2}\frac{\tau}{1+\tau^2\omega^2} \tag{3}$$

Here ΔN is the variance of carrier number and τ is the characteristic time of charge carriers. The spectrum of the fluctuations in Eq. (3) is a Lorentzian type curve. Fig. 3-1 shows an example of discrete modulation of current level through a submicron MOSFET in the time domain [29]. This type of spectrum is called random-telegraph-signal (RTS) noise or popcorn

noise. Fig. 3-2 shows a typical RTS noise curve in frequency domain, which is of the Debye-Lorentzian spectrum shape.

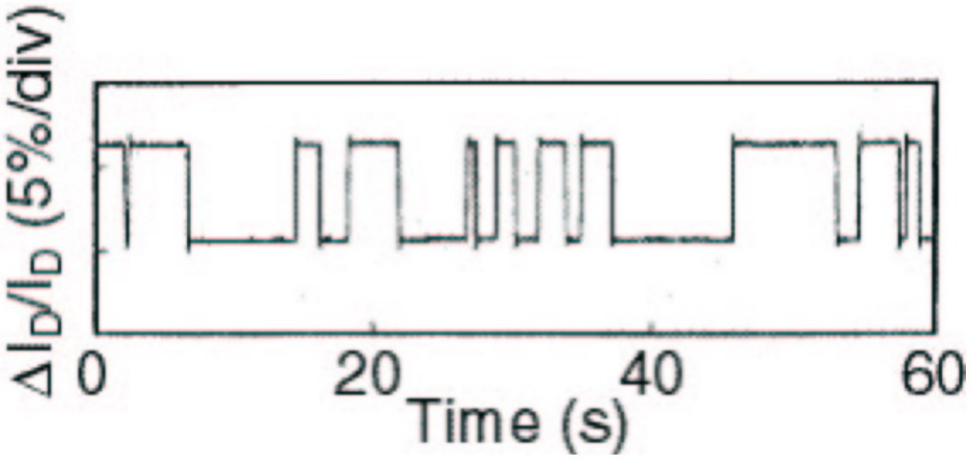

Fig. 2-2 Typical RTS noise, showing discrete levels of channel current modulation due to the trapping and release of a single carrier. (after [29])

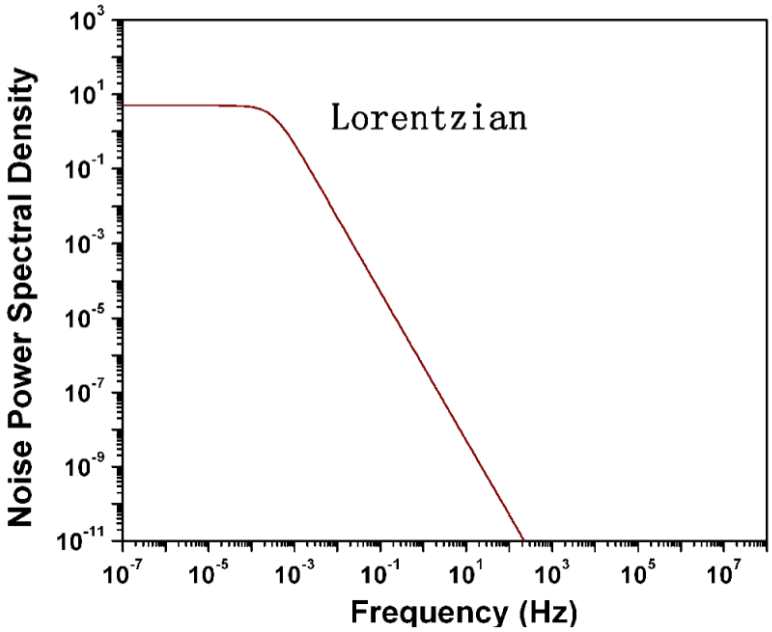

Fig. 2-3 A typical Debye-Lorentzian spectrum. (after [28])

b. 1/f noise

When a large number of traps exist in the device, several trapping/detrapping fluctuations happen over a range of tunneling times. The superposition of the effects of large numbers of defects similar to those leading to random telegraph noise could lead to 1/*f* noise in semiconductor devices [16]. Fig 2-4 shows the resistance fluctuation as a function of temperature and gate voltage (after [29]). At the lowest temperature, fluctuations turn out to be a random telegraph noise spectrum. A transition from random telegraph noise to 1/*f* noise is observed when increasing the temperature. In frequency domain, it works like several Lorentzian spectrums are added and each caused by separate tunneling time constants. The summation of these large numbers of uncorrected Lorentzian spectral gives 1/*f* type spectrum, as the example shown in Fig. 2-5.

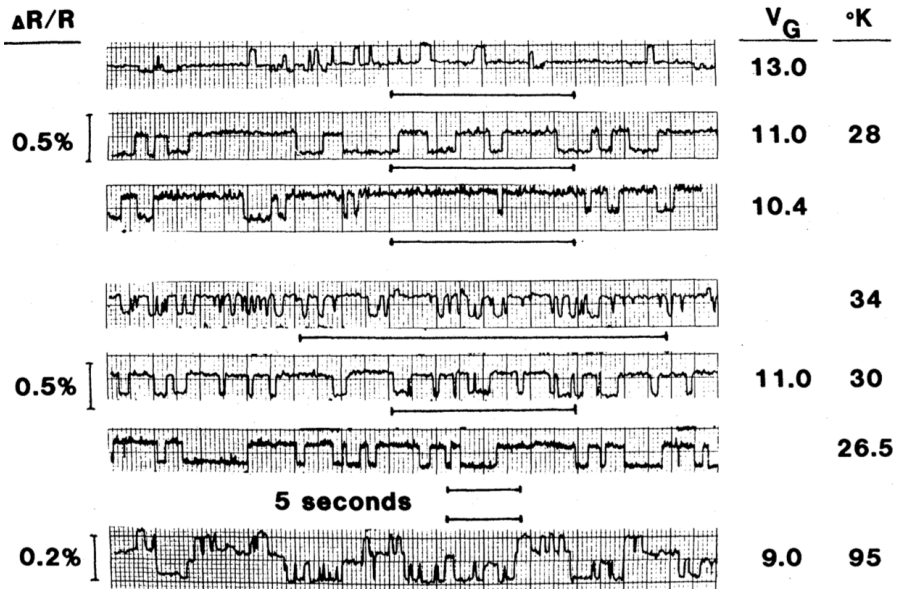

Fig. 2-4 Resistance switching observed in a small MOSFET in a particular range of temperatures and gate volt- ages. The last trace demonstrates that superposition can lead toward 1/*f* noise. (after [30])

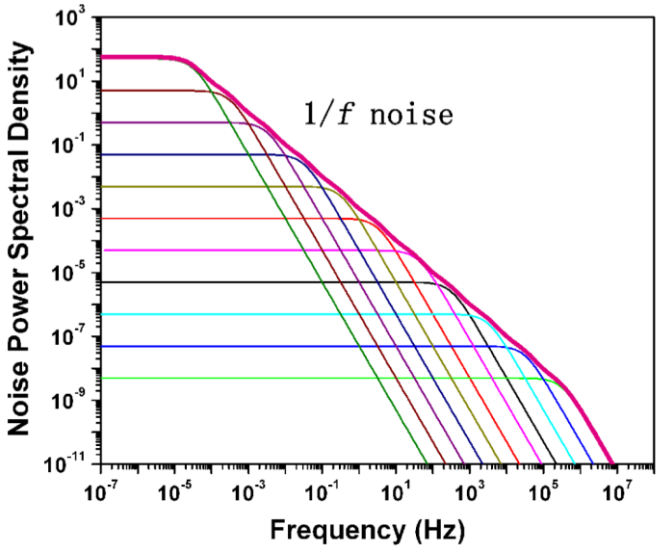

Fig. 2-5 1/*f* noise power spectral density can be obtained as a weighted summation of Lorentzians. Here ten Lorentzian spectra have been added, each with a characteristic time constant ten times higher than the previous one. (after [28])

According to the number fluctuation model, charge carriers tunneling between the channel and traps (typically in an adjacent dielectric layer) lead to fluctuations in trap occupancy, and consequently 1/*f* noise [25], [31]-[33]. For example, if a MOS device is operated in its linear region at constant drain current and gate bias, the 1/*f* noise can be described by:

$$S_{vd} = \frac{q^2}{C_{ox}^2} \frac{V_d^2}{(V_g - V_{th})^2} \frac{k_B T D_t(E_f)}{LW \ln(\tau_1/\tau_2)} \frac{1}{f} \tag{4}$$

Here S_{vd} is the excess drain-voltage noise power spectral density, V_{th}, V_g, and V_d are the threshold, gate, and drain voltages, f is the frequency, q is the electronic charge, C_{ox} is the gate-oxide capacitance per unit area, L and W are the transistor channel length and width, k_B is the Boltzmann constant, T is the absolute temperature, $D_t(E_f)$ is the number of traps per unit energy

per unit area at the Fermi level E_f, and τ_1 and τ_2 are maximum and minimum tunneling time, respectively [33].

Hooge's Mobility Fluctuation Model

The second model of low frequency noise is modeled from the fluctuation of the carrier mobility, which was first proposed by Hooge in 1969 [34], with an empirical formula for homogenous semiconductor devices and metals:

$$\frac{S_R}{R^2} = \frac{\alpha}{fN} \tag{5}$$

Here S_R is the noise power spectral density of resistance, N is the total number of carriers in the channel, and α is an empirical dimensionless value devices [34]. The mobility fluctuation model suggests that the low frequency noise of homogenous semiconductor devices is primarily caused by the lattice vibration [34].

In 1981, Hooge and collaborators extended the mobility model for homogeneous semiconductors to analyze the low frequency noise in MOSFET. They have attributed $1/f$ noise predominantly to a bulk effect, caused by fluctuations in the mobility of individual channel carriers [26]. The low-frequency noise in semiconductors and metals has been described by Hooge with the following popular, empirical expression:

$$\frac{S_V(f)}{V^2} = \frac{S_I(f)}{I^2} = \frac{S_R(f)}{R^2} = \frac{\alpha_H}{Nf} \tag{6}$$

Here α_H is the Hooge's constant, an empirical factor used to compare the noise of different kinds of microelectronic devices [26].

Noise Model of HEMT

For a HEMT, there are three regions of interest in a plot of S_{vd} vs. V_g - V_{th}, depending on applied gate bias, relative to V_{th}. As shown in the inset of Fig. 2-6, the channel resistance of HEMTs is the sum of two parts, the relatively constant resistance of the ungated region R_U, and the variable resistance of the gated region R_G. For a HEMT [9], [19]-[21]:

$$R_{total} = R_G + R_U = \frac{L_{gate} V_{th}}{W q \mu n_{ch} (V_g - V_{th})} + R_U \tag{7}$$

Here μ is the channel mobility, n_{ch} is the areal carrier density in the two dimensional electron gas (2DEG), L_{gate} is the length of the gated region of the channel, W is the channel width, and q is the electronic charge. In the Hooge's model of low frequency noise for a HEMT, the noise of the gated region of the transistor channel is expressed via Eq. (1) as [9], [19]-[21],[26]:

$$S_{Rtotal} = S_{RG} + S_{RU} = S_{RU} + \frac{\alpha_{ch} R_{ch}^2}{Nf} \tag{8}$$

For V_g very close to threshold, the carrier density is low in the gated region of the channel, the noise in the gated portion of the channel is the dominant noise source, and $R_G \geqslant R_U$. So the Hooge's model expression for the noise in this limiting case reduces to [9],[19]-[21]:

$$\frac{S_V}{V^2} = \frac{\alpha_{ch}}{Nf} \tag{9}$$

Because $N_{ch} \sim (V_g - V_{th})^{-1}$, the gate voltage dependence of the noise is anticipated in the Hooge's model to be:

$$S_{vd} = \frac{\alpha}{Nf} V_d^2 \propto (V_g - V_{th})^{-1} \tag{10}$$

This dependence is illustrated in Fig. 1 for small $v_g = (V_g - V_{th})^{-1}$.

At slightly more positive gate bias, relative to threshold, the density of electrons increases in the channel, and the noise still originates predominantly in the gated portion of the channel. But now $R_G << R_U$, and the Hooge model can be approximated as [9], [19]-[21]:

$$\frac{S_{vd}}{V^2} = \frac{S_{Rtotal}}{R_{total}^2} = \frac{\alpha R_G{}^2}{NfR_U^2} \propto (V_g - V_{th})^{-3} \tag{11}$$

This stronger voltage dependence is illustrated in Fig. 1 for intermediate values of $v_g = (V_g - V_{th})^{-3}$.

For still larger voltage magnitudes, both the resistance and noise are dominated by the ungated portion of the channel, and the noise becomes independent of gate bias [8],[18]-[20], where N_U is the total number of carriers in the ungated portion of the channel:

$$S_{vd} = \frac{\alpha V_d^2}{fN_U} \propto (V_g - V_{th})^0 \tag{12}$$

Hence, the noise in this region is expected to be relatively independent of gate voltage, as shown in Fig. 2-6.

For small values of $(V_g - V_{th})^{-1}$, where the Hooge model assumes S_{vd} is proportional to $1/N \sim (V_g - V_{th})^{-1}$, the number fluctuation model (Eq. 1) predicts that S_{vd} is proportional to $1/N^2$, and $S_{vd} \sim (V_g - V_{th})^{-2}$ for constant $D_t(E)$ [16],[17],[25],[35]-[37]. In the intermediate voltage region, where the Hooge model predicts the noise to scale as $(V_g - V_{th})^{-3}$, we expect for number fluctuations that the noise should analogously scale as $\sim (V_{gs} - V_{th})^{-4}$ when $D_t(E)$ is approximately uniform in energy [38]. For many semiconductor devices, the defect energy distribution is often not uniform [10]-[11],[16], so it is often difficult from a limited set of measurements to determine which model more accurately describes the $1/f$ noise of AlGaN/GaN HEMTs. In the following chapters, we will present a wide range of data for as-processed and proton-irradiated devices that enables

us to determine the origin of the noise that originates in the gated region of the channel, which is of most practical interest for HEMTs.

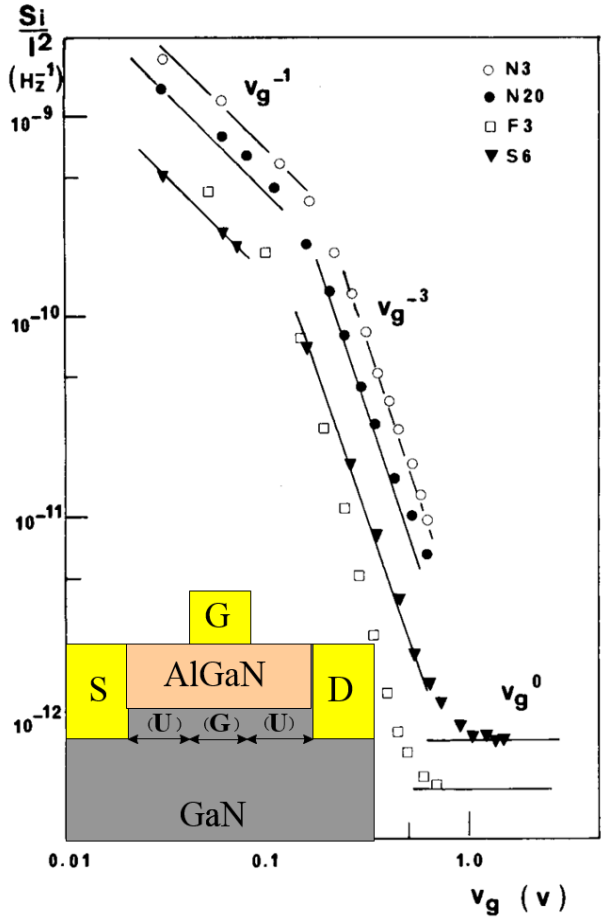

Fig. 2-6 Relative current noise power spectral density as a function of applied, effective gate voltage (here $v_g = (V_g - V_{th})^{-1}$), showing the approximate voltage dependences assumed in the Hooge mobility model of low-frequency noise in a number of differently processed HEMTs. (See Peransin et al. [21] for details, © IEEE, 1990). The inset is a schematic cross-section of a GaN HEMT, where the gated (G) and ungated (U) portions of the channel are labeled.

CHAPTER III

EXPERIMENTAL DETAIL

This chapter introduces the information of GaN HEMTs used and measurement techniques employed in this work. The settings of proton irradiation and biasing conditions are also provided.

Device Information

Three kinds of AlGaN/GaN HMETs built in different process technologies have been evaluated in this work. They are commercial GaN HEMTs fabricated by Qorvo, Inc., [39]-[40] and Cree, Inc., (Model number CGH40006P) [41], and high-quality, research-grade GaN HEMTs fabricated at University of California, Santa Barbara (UCSB) [42]. A schematic cross section of the GaN HEMTs fabricated at UCSB is shown in Fig. 3-1. AlGaN/GaN HEMTs were fabricated on AlGaN/GaN heterostructures grown by Ga-rich plasma-assisted molecular beam epitaxy (PAMBE) with 700 nm unintentionally doped (UID) GaN on GaN substrates grown by MOCVD on SiC [42], [43]. The gate has the shape of an inverted trapezoid, with a length (L_G) of 0.7 μm. The gate-to-drain separation (L_{GD}) is 1 μm and the gate-to-source separation (L_{GS}) is 0.5 μm [42]. Other two commercial parts have similar structure.

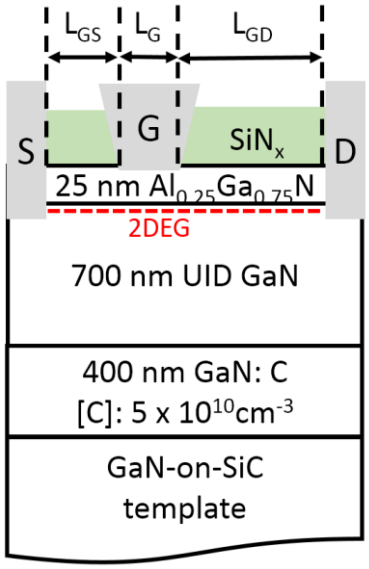

Fig. 3-1 Schematic cross-section of an AlGaN/GaN HEMT. (after [43])

DC Characteristics

DC measurements were performed using a HP4156B or Agilent B1505 parametric analyzer. Fig. 3-2 shows a typical I_d-V_g curves of AlGaN/GaN HEMTs (Qorvo devices), with drain to source voltage swept from 0 to 5 V at room temperature. The threshold voltage is about -3 V here. For other GaN HEMTs used in this thesis, the threshold voltage varies from -3 V to -4 V.

In this work, the range used for temperature dependence of low frequency noise is from 85K to 400 K. The DC characteristics of GaN HEMTs at this range of temperatures are also performed, with an example shown in Fig. 3-3. AlGaN/GaN HEMTs function well in this wide range of temperature. The threshold voltage shifts negatively with increasing temperature, indicating sheet carrier density decrease in this process. And the ON-state current decreases from 85 K to 400K, which is caused by smaller electron mobility in the 2DEG due to more scattering in the channel when heating the devices. As the threshold voltage changes with temperature, the gate bias is adjusted carefully when performing temperature dependence of low frequency noise.

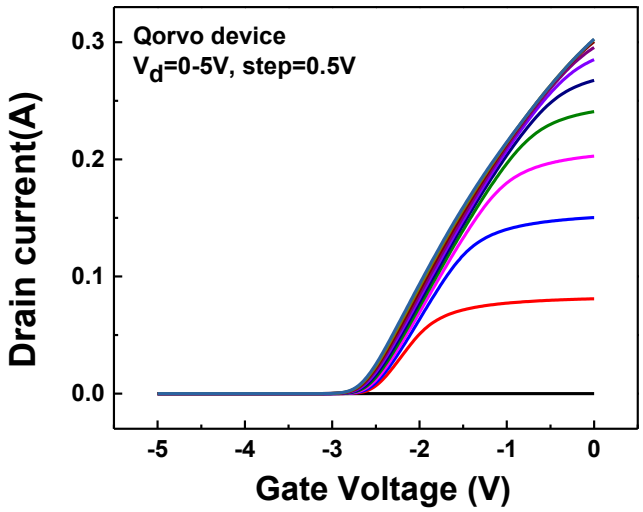

Fig. 3-2 DC characteristic: I_d-V_g curves for AlGaN/GaN HEMTs.

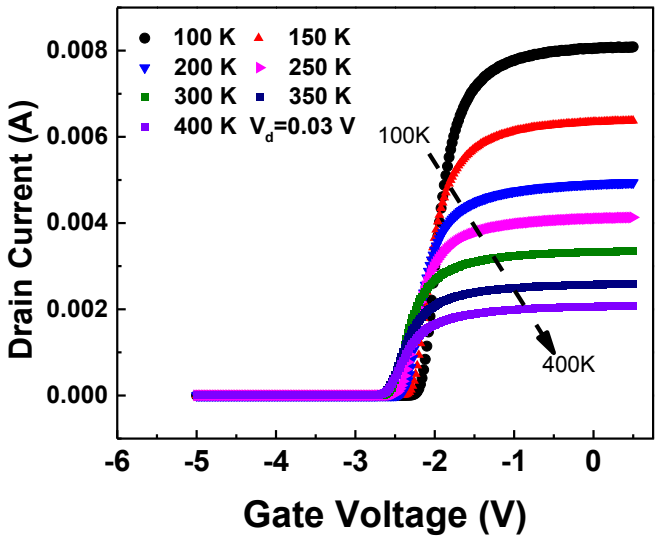

Fig. 3-3 I_d-V_g curves at different temperatures for Qorvo devices.

Low Frequency Noise Measurement

Excess noise measurements are performed on AlGaN/GaN HEMTs in strong inversion condition with apparatus shown in Fig. 3-4. During the noise measurement, both the gate and drain were D.C. biased and the substrate and source terminals were grounded. The drain current was derived from a constant voltage source in series with a large resistor to protect and keep drain bias. Another voltage source was connected directly to the gate terminal. Fluctuations in the drain to source voltage were first observed with a low noise pre amplifier before inputting into an FFT spectrum analyzer.

In this work, excess noise (corrected for background noise) was measured over a frequency span of 3 Hz to 390 Hz with drain biased at constant 0.03 V and substrate and source grounded.

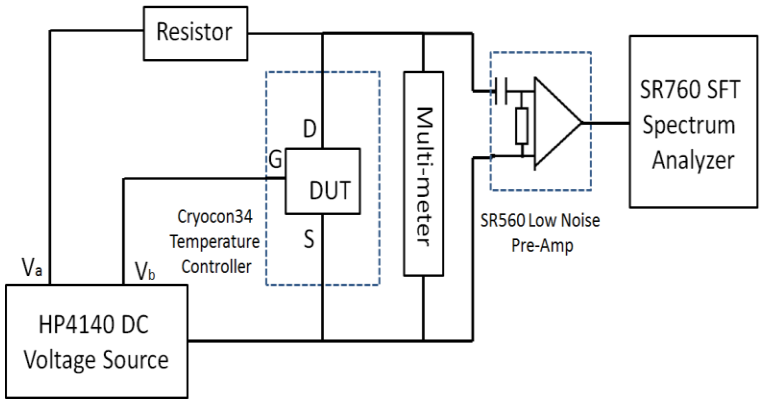

Fig. 3-4 Low frequency 1/*f* noise measurement system. (after [11])

Proton Irradiation

1.8 MeV of proton energy was chosen to study the displacement damage on the GaN HEMTs and compare with previous publications [8], [10], [11]. In this work, a fluence of $3x10^{13}/cm^2$ has been reached using the Vanderbilt Pelletron. During the proton irradiation, devices were put into the Pelletron chamber and biased under the following different conditions: 1) GND (V_{gs} = 0 V and V_{ds} = 0 V), 2) OFF (V_{gs} = -7 V and V_{ds} = 25 V), 3) semi-ON (V_{gs} = -2 V and V_{ds} = 25 V), and 4) ON (V_{gs} = +1 V and V_{ds} = 20 V). The irradiation is performed at room temperature. I_d-V_g response was monitored using an Agilent B1505 parametric analyzer during the irradiation process. 1/*f* noise measurement was performed before and after irradiation.

CHAPTER IV

LOW FREQUENCY NOISE VS. PROTON IRRADIATION

In this chapter, the radiation response of 1.8 MeV proton irradiation was evaluated firstly. The frequency dependence and gate bias dependence of low frequency noise before and after irradiation were studied in detail. The results indicated that the noise was more consistent with a number fluctuation model, rather than the Hooge mobility fluctuation model often applied to AlGaN/GaN HEMTs. The variations in frequency exponent and gate bias suggested the non-uniformity of the trap distribution in these devices.

Radiation Response

Many previous irradiation studies suggest that the GaN based devices are extremely radiation hard and proton energy has a strong effect on the amount of damage created in the HEMTs [8],[44]-[47]. In this work, all the GaN HEMTs were subjected to 1.8 MeV proton irradiation and the DC characteristics were performed before and after irradiation. Fig. 4-1 shows the I_d-V_g curves for AlGaN/GaN HEMTs from Qorvo, Inc, before and after proton irradiation under Semi-On bias condition. A positive threshold voltage shift is observed after proton irradiation, which suggests that the acceptor-like traps created during the irradiation. After a fluences of 3 x 10^{13} cm^{-2}, the threshold voltage shifts about 0.25 V. The On state current decreases after irradiation, suggesting that the creation of deep acceptor-like traps.

Fig. 4-2 summarizes the V_{th} shifts and degradation of the normalized peak g_m for GaN HEMTs manufactured by Qorvo, Inc., as a function of proton irradiation under different biases.

For the samples from Qorvo, Inc. in Fig. 4-2 (a), the largest V_{th} shift (~ 0.3 V increase) and gm reduction (~ 17% decrease) after proton irradiation to a fluences of 3 x 10^{13}/cm^2 are observed for the semi-ON bias condition. Voltage stress without irradiation leads to a V_{th} shift of less than 50 mV and gm degradation of less than 2%, as shown in Fig. 4-2; hence, the primary changes in device characteristics are associated with the proton exposure.

For the samples from UCSB, the worst case response to proton irradiation is instead observed under ON bias, as demonstrated in [43]. Fig. 4-3 shows that the peak gm degrades about 15% and V_{th} shifts about 0.2 V at a fluence of 10^{14} cm^{-2} when devices are irradiated under ON bias. For both Qorvo and UCSB samples, positive shifts in V_{th} are observed, indicating that acceptor-like defects are created during proton irradiation, which in these types of devices are primarily N-vacancy-related defects and O-related impurity centers [8]-[11].

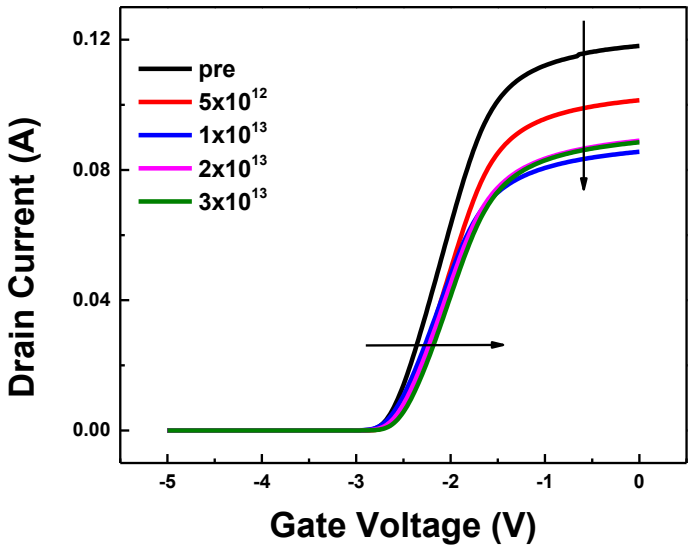

Fig. 4-1 I_d-V_g characteristics after 1.8 MeV proton irradiation. The measurement is taken at V_{ds} = 5 V. Fluences are quoted in protons/cm^2.

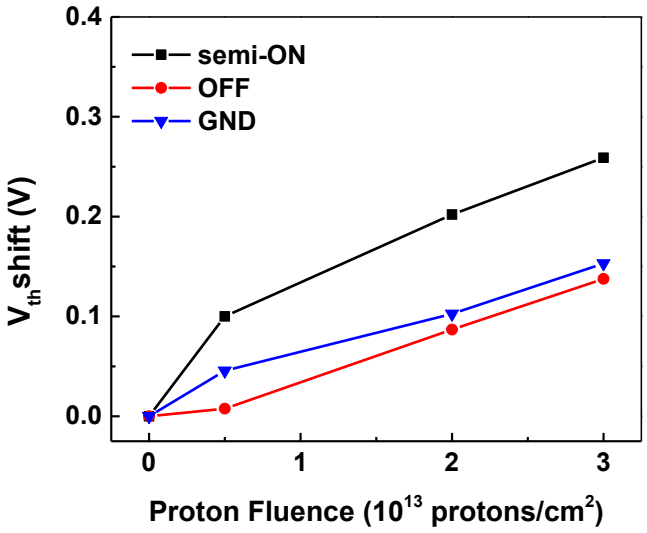

(a)

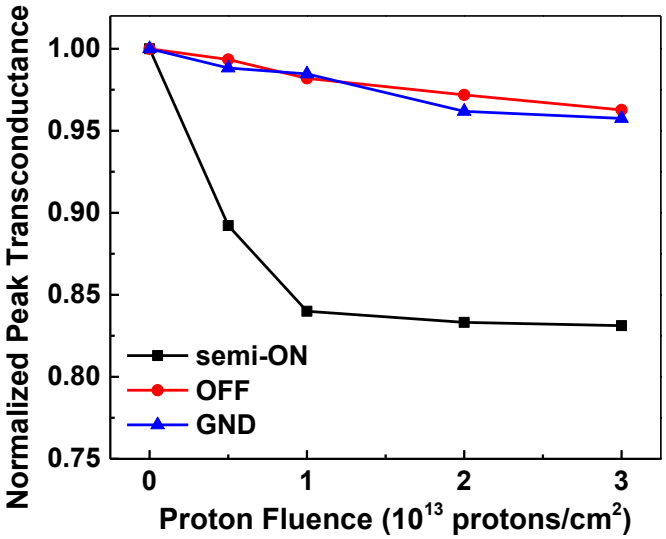

(b)

Fig. 4-2 (a) V_{th} shift and (b) normalized peak transconductance for AlGaN/GaN HEMTs with 0.25 µm gate length, and ~ 100 µm channel width from Qorvo, Inc., as a function of proton fluence. V_{ds} = 5 V during measurement. (after [38])

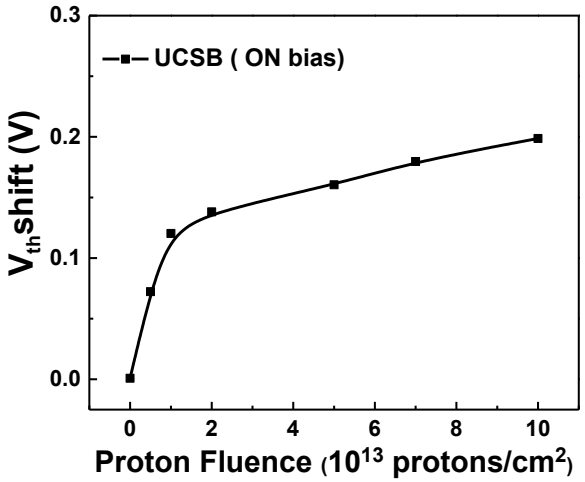

(a)

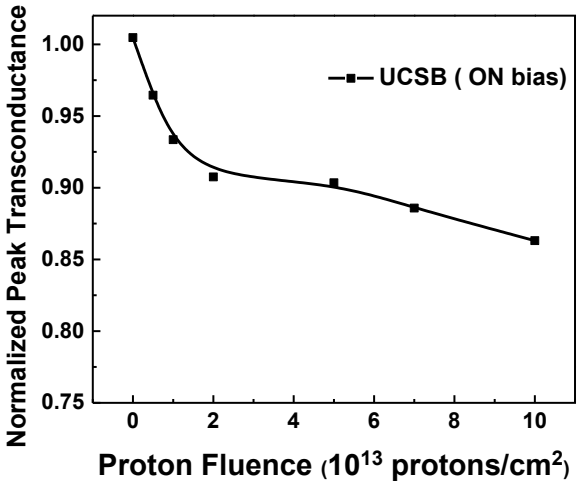

(b)

Fig. 4-3 (a) V_{th} shift and (b) normalized peak g_m for AlGaN/GaN HEMTs with a gate length of 0.7 μm and width of 150 μm from UCSB, irradiated under ON bias, as a function of proton fluence. V_{ds} = 5 V during measurement. (after [38])

Frequency Dependence of 1/f noise

Fig. 4-4 shows an example of excess drain voltage noise power spectral density S_{vd} (corrected for background noise) for AlGaN/GaN HEMTs at constant V_g - V_{th}=0.4 V and V_d =

0.03 V as a function of frequency at room temperature. Devices differ in dimensions and process technology, leading to different room-temperature noise magnitudes. Note that the noise of the UCSB devices follows a $1/f$ power law more closely than the Qorvo and Cree devices shown here, so for much of the analysis that follows, the noise is monitored in more than a single frequency range, to ensure that the conclusions are not significantly affected by the frequency chosen for the voltage dependence and radiation response results that follow.

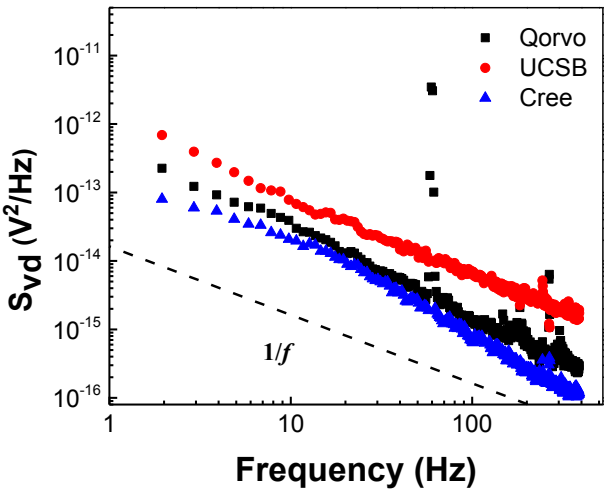

Fig. 4-4 Excess voltage-noise power spectral density as a function of frequency for three GaN HEMTs fabricated in different process technologies at 295 K. V_g - V_{th} = 0.4 V, and V_d = 0.03 V. (after [38])

Fig. 4-5 shows S_{vd} versus frequency f for noise measurements on Qorvo devices at constant V_g - V_{th} = 0.4 V and V_d = 0.03 V, before and after irradiation to a fluence of 3 x 10^{13} protons/cm^2 under worst case, semi-ON bias. Before irradiation, the slope of the frequency dependence $\alpha = -\partial \ln S_{vd}/\partial \ln f = 0.90 \pm 0.05$ for the lower-frequency range, 2 Hz < f < 20 Hz, and $\alpha = 1.40 \pm 0.05$ for the higher-frequency range, 20 Hz < f < 300 Hz. After proton irradiation to a fluence of 10^{13}/cm^2, α is still 0.90 ± 0.05 for the lower-frequency range, but decreases to

1.30 ± 0.05 for the higher-frequency range. Further exposure to a proton fluence of $3x10^{13}/cm^2$ reduces α slightly to 0.85 ± 0.05 for the lower-frequency range and 1.25 ± 0.05 for the higher-frequency range.

Neither the changes in $\alpha = -\partial \ln S_{vd}/\partial \ln f$ with frequency nor the reductions in magnitude of $\alpha_H = S_{vd}Nf/V^2$ that result from proton irradiation are easily described within the framework of the mobility-fluctuation noise model that is often applied to AlGaN/GaN HEMTs [8],[22]-[24]. Physically, this is because, up to at least proton fluences of ~ 10^{15} to 10^{16} /cm^2 (i.e., as long as the basic GaN lattice structure remains intact), carrier-phonon scattering in bulk GaN is not affected nearly as strongly by proton irradiation as is defect-related charge trapping [48]. In contrast, number-fluctuation noise caused by defects with a non-uniform $D_t(E)$ often leads to similar changes in frequency response as observed here [11],[13],[17],[49]-[54].

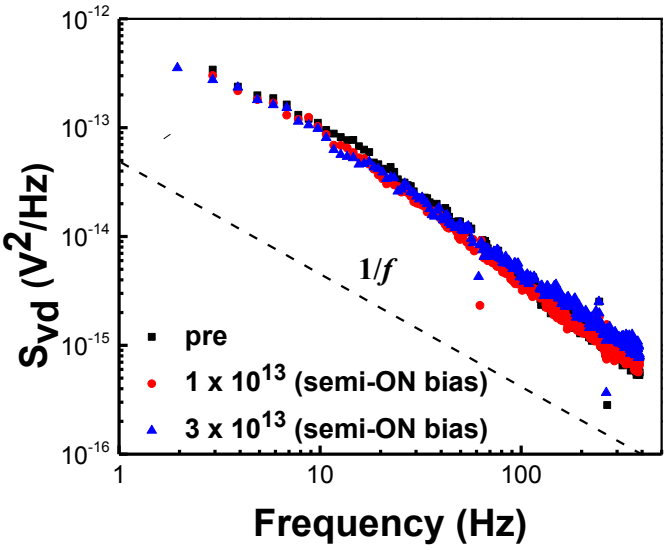

Fig. 4-5 S_{vd} as a function of frequency for Qorvo devices before and after the devices were irradiated with 1.8 MeV protons to a fluence of up to 3 x 10^{13}/cm^2. Devices were biased under the semi-on condition. V_d = 30 mV and V_g = 0.4 V during the noise measurements. Fluences are quoted in protons/cm^2. (after [38])

Gate Voltage Dependence of 1/f Noise

Fig. 4-6 shows S_{vd} as a function of frequency for several gate bias conditions. All are typical low frequency noise spectrum and S_{vd} decreases with increasing gate bias. Fig. 4-7 shows S_{vd} as a function of V_g-V_{th} at 10 Hz and room temperature for three kinds of GaN HEMTs prior to irradiation. While the slopes of the curves, β_1 and β_2 (defined in Fig. 4-7), may appear superficially to follow the trends illustrated in Fig. 2-6, significant deviations from the simple mobility-fluctuation predictions are observed in some cases.

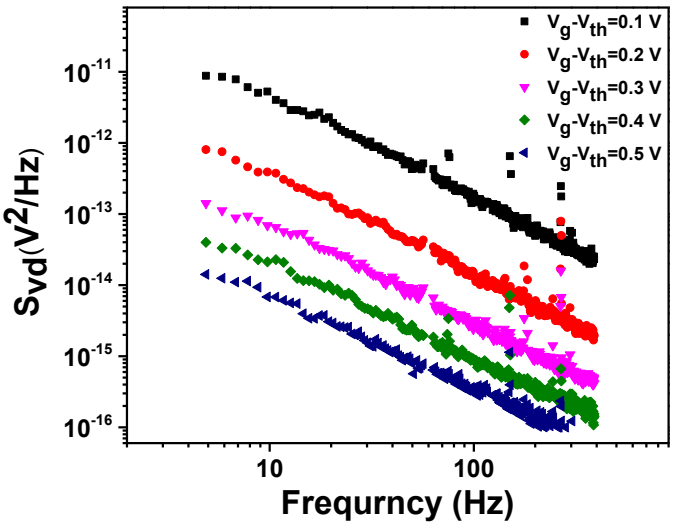

Fig. 4-6 S_{vd} as a function of frequency for different gate biases, V_d = 0.03V.

For these unirradiated devices, for voltages very close to threshold, β_1 = 1.0 ± 0.1 for the USCB devices; 1.2 ± 0.1 for the Qorvo devices, and 0.9 ± 0.2 for the Cree devices. For higher voltages, β_2 = 3.2 ± 0.1 for the UCSB devices; 3.9 ± 0.2 for the Qorvo devices; and 3.8 ± 0.1 for the Cree devices. That four of these six measurements appear to be more consistent with the mobility fluctuation model than the number fluctuation model (assuming constant defect-energy distribution) is one factor that accounts for the popularity of the mobility fluctuation model in

previous studies of the low-frequency noise of AlGaN/GaN HEMTs [8],[19]-[24] [26]. However, the totality of the evidence presented here and elsewhere [13],[16],[25],[49]-[54] strongly suggests this agreement is almost certainly fortuitous.

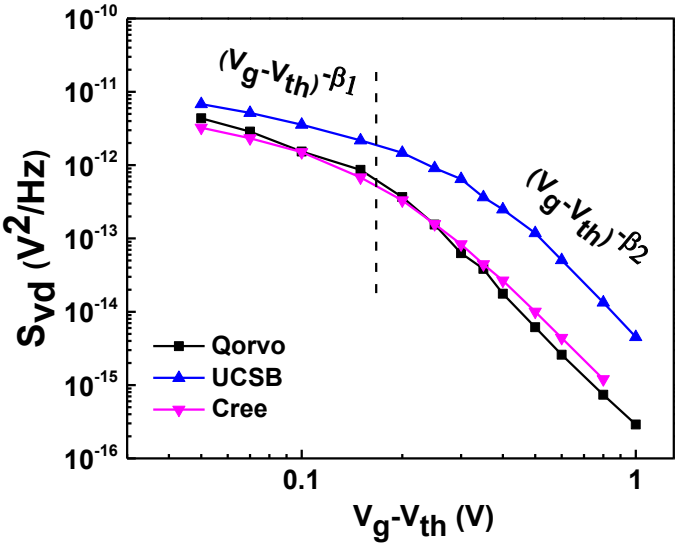

Fig. 4-7. S_{vd} at 10 Hz and room temperature as a function of V_g–V_{th} for three unirradiated GaN HEMTs fabricated in three different process technologies. V_d = 0.03 V. (after [38])

Fig. 4-8 shows the gate voltage dependence of S_{vd} before and after proton irradiation for Qorvo devices under (a) semi-ON, (b) GND, and (c) OFF bias conditions, and Fig. 4-9 shows the results for UCSB devices irradiated under ON bias. Because there is not a uniform frequency dependence of the noise for these devices as we show before, we plot S_{vd} at both 10 Hz (representative of the lower frequency range) and 100 Hz (representative of the higher frequency range) as functions of $V_g - V_{th}$.

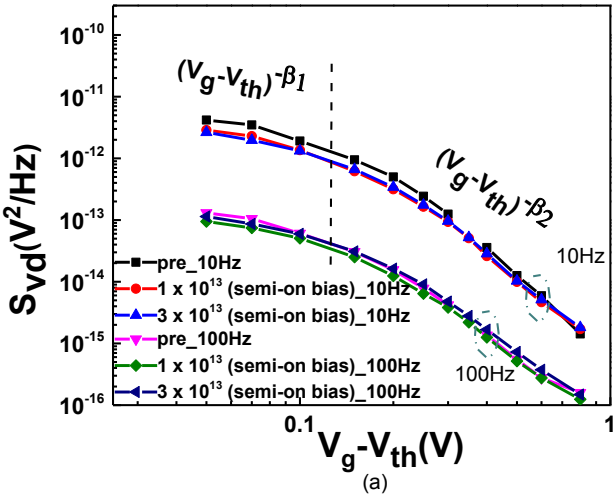

(a)

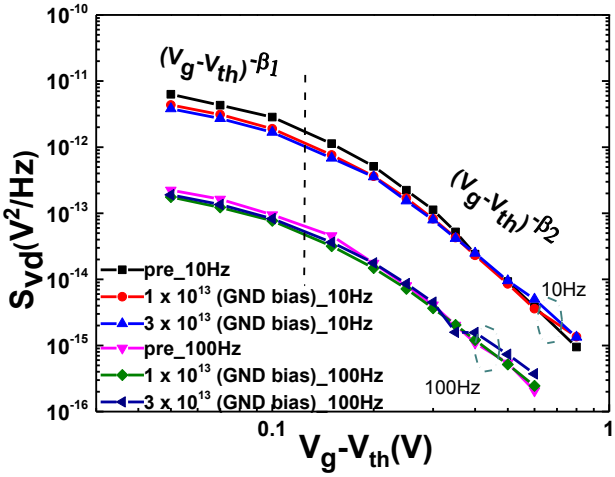

(b)

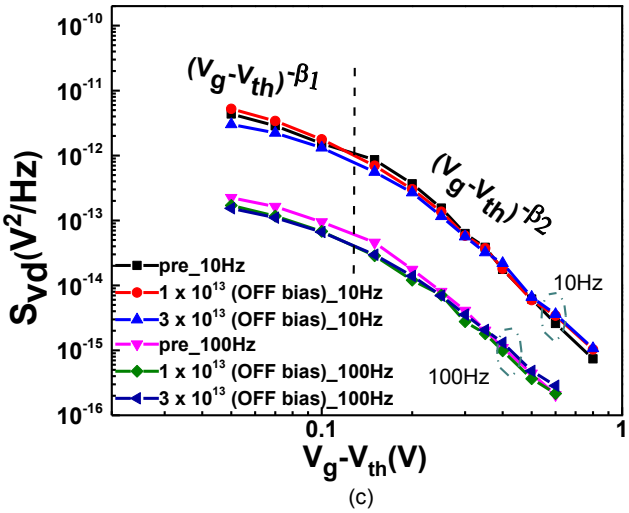

(c)

Fig. 4-8. S_{Vd} at 10 Hz and 100 Hz as a function of V_g–V_{th} for AlGaN/GaN HEMTs before and after proton irradiation up to 3 x 10^{13}/cm^2 for Qorvo devices biased under the (a) semi-ON condition (b) grounded bias conditions, (c) OFF-state condition. V_d = 30 mV during the noise measurements. (after [38])

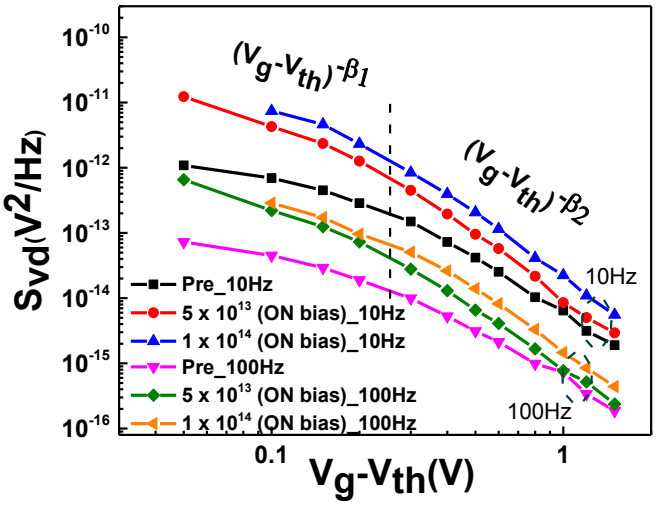

Fig. 4-9 S_{vd} at 10 Hz and 100 Hz as a function of $Vg–Vth$ for AlGaN/GaN HEMTs before and after proton irradiation up to 1 x 10^{14} /cm^2 for UCSB devices biased under the ON condition (V_g = +1 V and V_{ds} = 20 V); V_d = 30 mV during the noise measurements. (after [38])

Figs. 4-10 and 4-11 summarize variations of the voltage-dependence slopes β_1 and β_2 with bias during irradiation and proton fluence for the results of Figs. 4-8 and 4-9, as well as the predictions of the mobility fluctuation model. For Qorvo devices, values of β_1 in Figs. 7 and 8 vary from ~ 0.9 to 1.3, depending on the applied bias, and generally *decrease* with proton fluence. Values of β_2 vary from ~ 3.4 to 4.0, and also generally decrease with proton fluence. For the UCSB devices in Fig. 4-9, values of β_1 vary from ~ 0.9 to 1.5, depending on the applied gate bias during noise measurement, and generally *increase* with proton fluence. Values of β_2 vary from ~ 2.9 to 3.3, and also generally increase with proton fluences.

Neither the deviations from the expected values of β_1 = 1.0 and β_2 = 3.0 nor the changes in values of β with irradiation can be explained easily via the standard Hooge mobility model. Similar deviations from the mobility-fluctuation model predictions also have been identified in other devices [8],[55] that we have re-evaluated (not shown here), as part of this study. Instead,

the noise is consistent with number fluctuations, with $D_t(E_f)$ that are non-constant in energy before and after irradiation [10],[11].

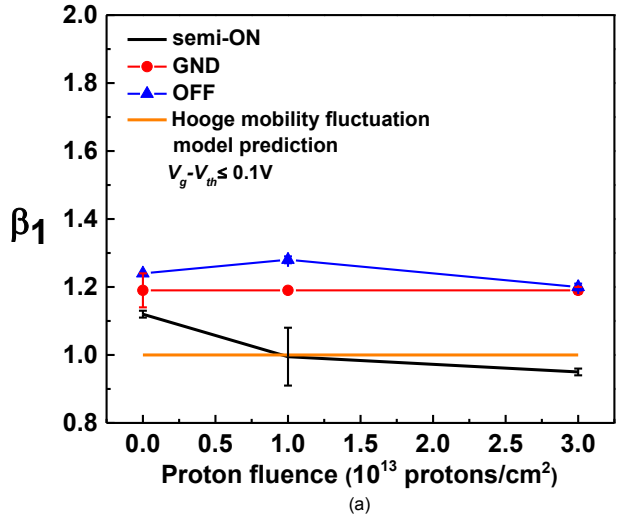

Fig. 4-10. Summaries of (a) β_1 and (b) β_2 for GaN HEMTs as a function of proton fluence and irradiation bias conditions, summarizing the data of Figs. 4-8(a)-(c). In each case, estimates obtained for the curves in Figs. 4-8 for f = 10 Hz and f = 100 Hz are averaged, so error bars provide estimates in variation of the gate-voltage dependence exponent β with measuring frequency. Also shown are predicted responses based on the Hooge mobility fluctuation model. (after [38])

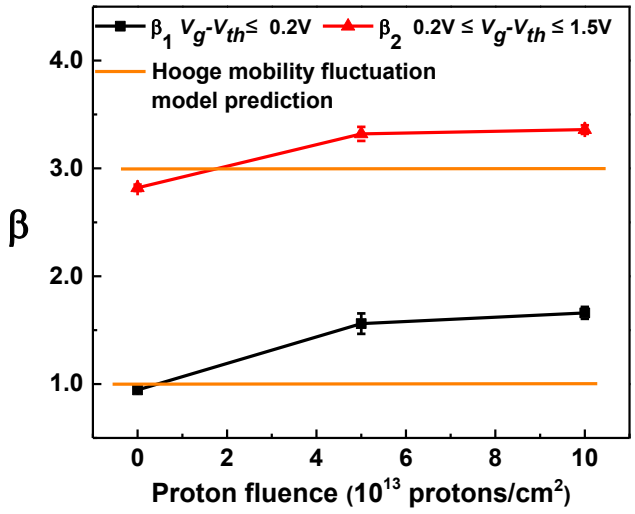

Fig. 4-11. Summaries of β for GaN HEMTs from UCSB as a function of proton fluence and irradiation bias conditions, summarizing the data of Fig. 4-9. Also shown are predictions based on the Hooge mobility fluctuation model. (after [38])

It is often useful to examine the input-referred noise for a transistor [36],[55]. For a HEMT, as well as for a MOSFET, the input-referred gate voltage noise power spectral density $S_{vg} = S_{vd}(V_g - V_{th})^2/V_d^2$. For number fluctuation noise in a MOSFET, with a uniform defect-energy distribution, $D(E_o)$, S_{Vg} is approximately constant vs. $V_g - V_{th}$. By analogy, for a HEMT with a uniform defect-energy distribution, we would expect S_{vg} to be approximately constant for voltages close to threshold, and fall off inversely with $(V_g - V_{th})^2$. Values of S_{vg} extracted from Figs. 4-8(a) and 4-9 are shown in Fig. 4-12 as a function of gate voltage.

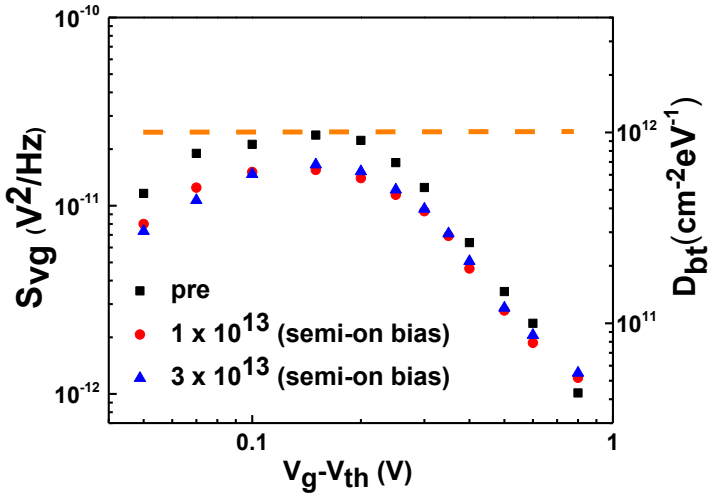

(a)

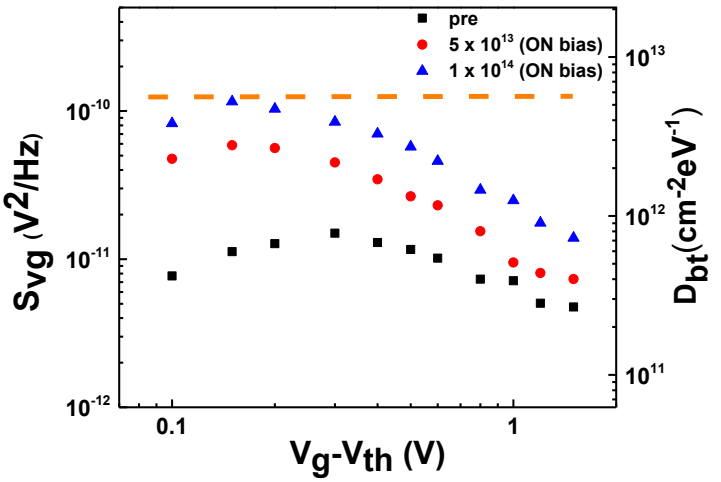

(b)

Fig. 4-12. Excess gate voltage noise power spectral density S_{vg} as a function of V_g-V_{th} at room temperature (a) for proton irradiation of Qorvo devices in the semi-ON condition, and (b) for proton irradiation of UCSB devices in the ON condition. The dashed lines mark the maximum noise levels of the devices near threshold. (after [38])

The right-hand y-axis in Fig. 4-12 shows the inferred, effective border trap defect energy distribution $D_{bt}(E)$ inferred from Eq. (4) at f =10 Hz. Here the value of "C_{ox}" in Eq. (4) is instead

the AlGaN barrier layer capacitance per unit area; the thickness of the barrier layer is about 25 nm, and the relative permittivity of AlGaN layer is ~ 9 [57]. Values of L and W are listed above, and we assume $\tau_1/\tau_2 \approx 10^{12}$ to be consistent with previous work [15],[43]. The dashed lines mark the maximum noise levels and effective border-trap densities of the devices near threshold at the highest proton fluences. The decrease in $D_{bt}(E)$ for small values of $V_g - V_{th}$ is evidence of a non-constant defect-energy distribution [16],[49], as discussed further below. The deviations at more positive voltages occur primarily because of the voltage divider discussed in Section II above. As a result of this voltage divider, only values of $D_{bt}(E)$ that are within ~100-200 mV of V_{th} have physical significance.

Current Noise vs. I and g_m

We have also applied the method of Ghibaudo et al. to analyze the low-frequency noise of these devices; this technique is based on evaluating the gate-input referred noise over a wide range of channel current [36]. For low-frequency noise in electronic devices due to equilibrium resistance fluctuations, as is the case here, $S_{Vd}/V_d^2 = S_I/I^2 = S_R/R^2$ [16]-[18], [26]. As noted above, noise caused by bulk mobility fluctuations should decrease linearly with I [36], while number-fluctuation noise in the simplest case of a constant defect-energy distribution $D_t(E_f)$ should decrease with I^2 [16],[26]. Fig. 13 shows S_I/I^2 as a function of drain current for as-processed Qorvo, Cree, and UCSB devices. Clearly, the curves are not linear; a quadratic dependence provides a close fit, with deviations at the lowest currents (close to threshold), consistent with trends in Figs. 9-12. Hence, the results of Fig. 13 are more consistent with number-fluctuation noise than mobility-fluctuation noise.

For noise due to number fluctuations, in cases where the defect-energy distribution is relatively uniform, one would also expect $S_{vd}/V_d^2 = S_I/I^2$ to be proportional to $(g_m/I_d)^2$ [36]. We check this proportionality in Fig. 14 for Qorvo devices, before and after proton irradiation. We see generally good agreement, with again deviations from perfect correlation that result most likely from non-uniformities in the defect-energy distribution, as confirmed in the next chapter.

The results of Figs. 13 and 14 are consistent with the work of Silvestri, et al. in [54], but are not consistent with the results and/or explicit or implicit assumptions of many other studies [8], [19]-[23]. These discrepancies occur at least in part because the method of Ghibaudo et al. [36],[56], while quite useful, can lead to ambiguous results any time that the defect energy distribution is increasing toward the relevant band edge, as is often the case in AlGaN/GaN HEMTs and other semiconductor devices, e.g., *p*MOS Si-based transistors, as discussed in [49],[54].

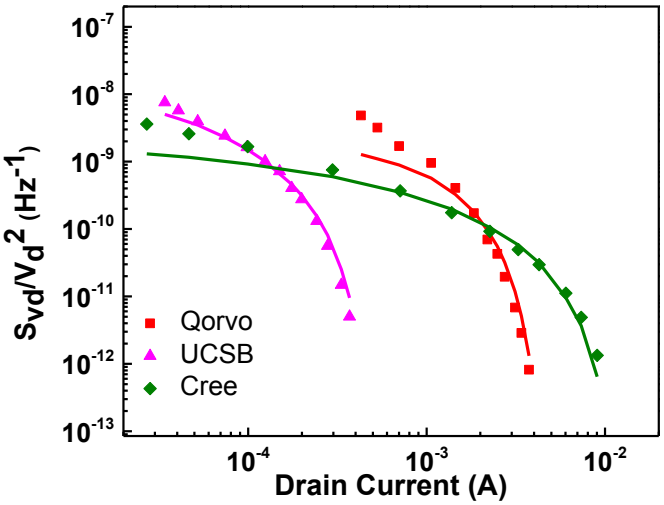

Fig.4-13. Normalized current spectral noise density S_I/I^2 at 10 Hz as a function of drain current for different kinds of GaN HEMTs, prior to proton irradiation. (after [38])

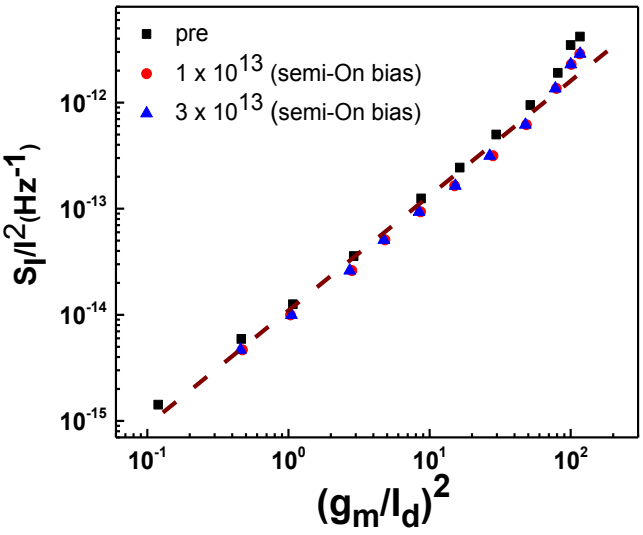

Fig. 4-14. Normalized drain-current noise-power spectral density S_I/I^2 at 10 Hz as a function of $(g_m/I_d)^2$ for Qorvo devices during proton irradiation, with devices biased in the semi-on condition. (after [38])

Conclusions

In this chapter, we evaluated the frequency and gate bias dependence of AlGaN/GaN HEMTs built in both commercial process and development stage process. Neither the voltage nor the frequency dependences of the observed low frequency noise can be explained by the popular Hooge mobility fluctuation model, but are well explained by a number fluctuation model with a non-constant defect-energy distribution.

CHAPTER V

LOW FREQUENCY NOISE VS. TEMPERATURE

Last chapter presents the low frequency noise results at room temperature. In this chapter, the gate voltage dependence of low frequency noise at various temperatures will be shown. The temperature dependent noise measurement was also performed to provide helpful information about the defect energy distribution in these devices. These results further confirmed the 1/*f* noise of AlGaN/GaN HEMTs originated from the carrier number fluctuations with a strongly non-uniform *D(E)* in these devices.

Gate Voltage Dependence of 1/f Noise

As shown in Fig. 3-3, the AlGaN/GaN HEMTs work well in the temperature range from 85 K to 400 K. Since the threshold voltage shift negatively with increasing temperature, the gate voltage is adjusted at different temperatures to keep a fixed increment from the threshold voltage to keep the electric fields remain approximately constant in the devices. Fig. 5-1 plots the excess drain-voltage noise power spectral density S_{vd} for GaN HEMTs at constant $V_g - V_{th} = 0.25$ V, and $V_d = 0.03$ V as a function of frequency and temperatures. All of these curves are typical low frequency noise curves, with noise varies approximately inversely with frequency.

The gate voltage dependence of low frequency noise at a wide range of temperature were performed as shown in Fig. 5-3 for AlGaN/GaN HEMTs from Qorvo, Inc. The gate voltage dependence slopes of the curves, β_1 and β_2 (defined in the same way as in chapter 4) look superficially follow the trend illustrated in Fig. 2-6 at these various temperatures. The values of

β_1 and β_2 were summarized from Fig.5-3 and shown in Fig. 5-4. The value of β_1 varies from ~0.9 to 1.5 and the β_2 varies from ~3.9 to 4.3. Significant deviations are also observed in some cases.

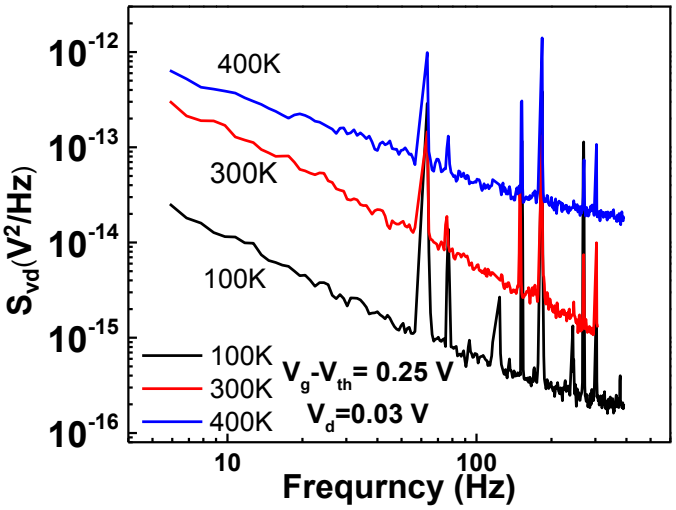

Fig. 5-1 S_{vd} as a function of frequency at 100K, 300K and 400K.

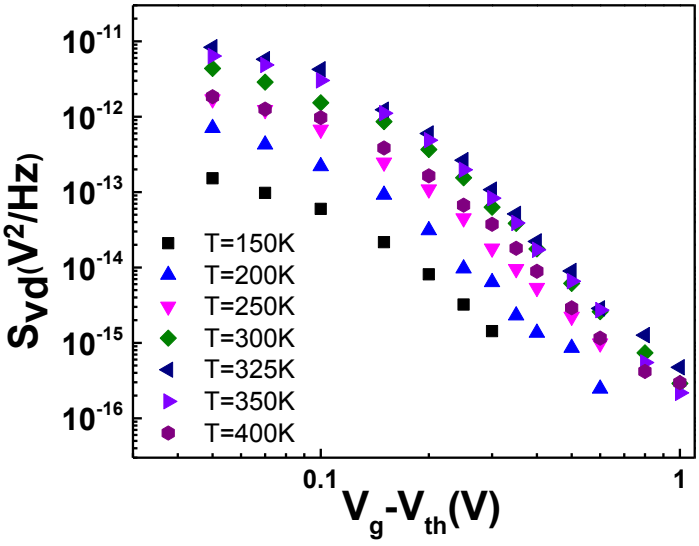

Fig. 5-2 Gate voltage dependence of S_{vd} as a function of temperature. V_d = 0.03V.

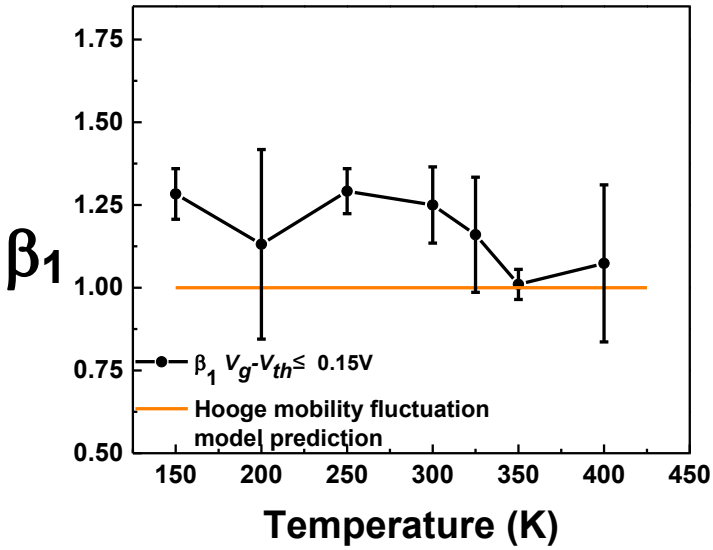

(a)

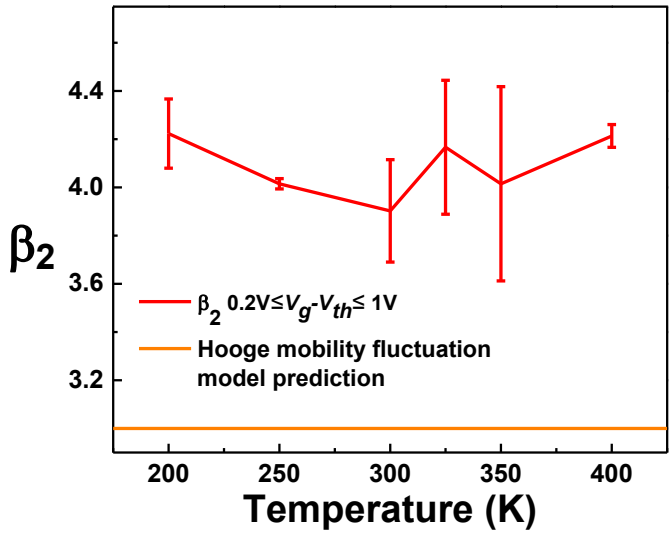

(b)

Fig. 5-3 Summaries of (a) β_1 and (b) β_2 for GaN HEMTs as a function of temperature, summarizing the data of Figs. 5-3. In each case, estimates obtained for the curves in Figs. 5-3 for f = 10 Hz and f = 100 Hz are averaged, so error bars provide estimates in variation of the gate-voltage dependence exponent β with measuring frequency. Also shown are predicted responses based on the Hooge mobility fluctuation model.

Again neither the values of the slopes at different temperatures nor the changes of β_1 and β_2 can be explained by the standard mobility fluctuation model. These noise results are more consistent with number fluctuation model, with non-constant defect energy distribution in energy, which is confirmed by previous discussion.

Similar to Fig. 4-14, the normalized drain current spectral density S_{vd}/V_d^2 at 10 Hz extracted from Fig. 5-3 as a function of $(g_m/I_d)^2$ and temperature was shown in Fig. 5-5. The observed strong correlation once again indicates that low frequency noise can be modeled by the carrier number fluctuation model associated with the trapping and detrapping of charges in defects near the interface.

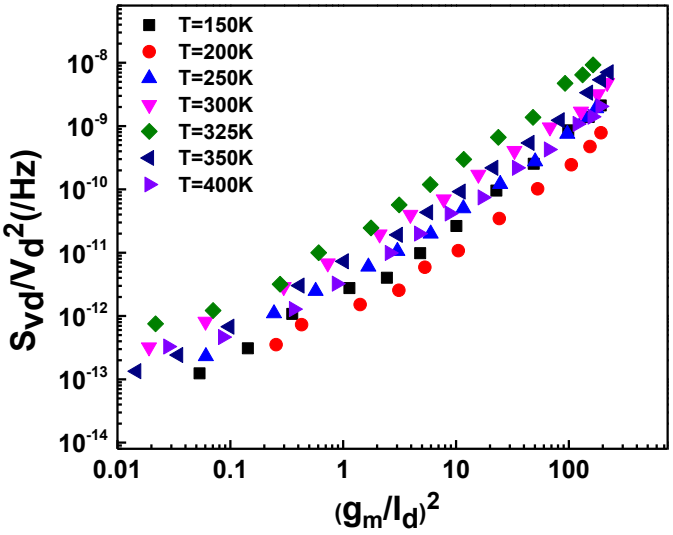

Fig. 5-4 Normalized drain-current noise-power spectral density S_I/I^2 at 10 Hz as a function of $(g_m/I_d)^2$ for Qorvo devices as a function of temperatures.

The frequency exponent was extracted from three samples as a function of gate bias and temperature, as shown in Fig.5- 6. The frequency exponent decreases with increasing gate bias

from 1.45 to 1.13. Again, such a dependence of α with gate bias can be explained a carrier fluctuation model in which there is a non-uniform trap distribution [10], [16], [58],

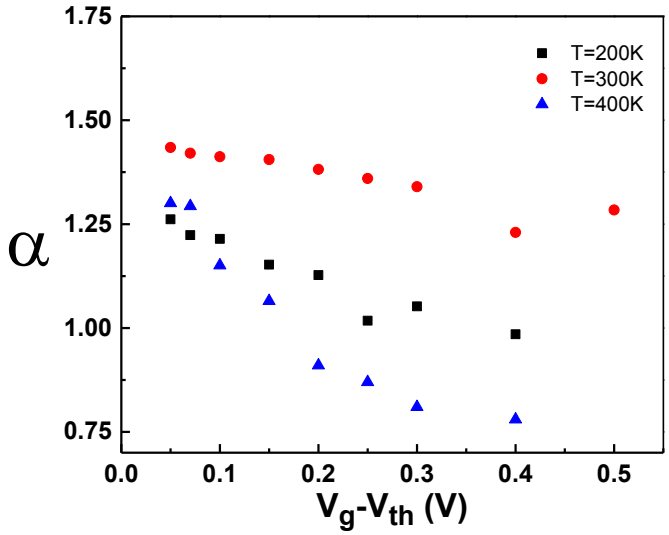

Fig. 5-5 Frequency exponent as a function of gate bias and temperatures.

Temperature Dependence of 1/f Noise

If the gate voltage dependence of the 1/*f* noise at room temperature arises from a non-uniform $D_t(E)$, then manifestations of the non-uniform $D_t(E)$ must also show up in the temperature dependence of the noise [16]-[18],[53], since each measurement probes a similar $D_t(E)$. Accordingly, Fig. 15 shows the temperature dependence of the low frequency noise of unirradiated UCSB and Qorvo devices. Close agreement is observed between the experimental data and predictions of the Dutta-Horn model [10],[11], confirming that defect-related noise dominates over bulk mobility fluctuation noise in these devices [16]-[18]. First-order estimates of the magnitudes of $D_{bt}(E)$ are shown on the right-hand y-axis, derived from Eq. (1) under the assumptions defined above. For each type of device, the normalized low frequency noise

increases significantly with temperature at ~ 300 K, confirming that $D_{bt}(E)$ is not constant in the vicinity of room temperature, but instead is changing rapidly. This rapid change in $D_{bt}(E)$ is consistent with the idea that these AlGaN/GaN HEMTs have a strongly varying defect-energy distribution after device processing [10],[11],[59],[60], which in turn leads to differences in the voltage dependence from expectations based on a constant $D_{bt}(E)$ [22],[36].

The variations in frequency and gate voltage dependence observed for the AlGaN/GaN HEMTs in Figs. 2-14 are quite similar to those observed in previous, detailed studies of the voltage dependence of the noise of irradiated and unirradiated Si MOSFETs [12],[33],[49], which are most easily interpreted as number-fluctuation noise with a significantly non-uniform $D_t(E)$. Moreover, this conclusion is also consistent with detailed studies of the temperature dependence of the noise of several different types of *irradiated* AlGaN/GaN HEMTs in previous work by Chen et al. [10], [11].

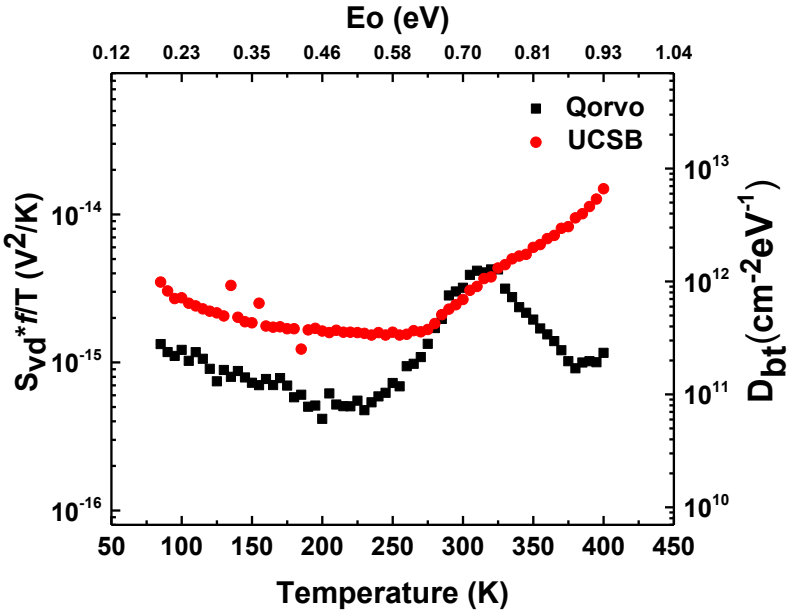

Fig. 5-6 Normalized noise from 85 K to 400 K for Qorvo and UCSB devices. Here $V_g - V_{th} = 0.4$ V, and $V_d = 0.03$ V at $f = 10$ Hz. The energy scale on the upper x-axis is based on the Dutta-Horn model of $1/f$ noise, and the right y-axis $D_{bt}(E)$, calculated from Eq.(4) (after [38])

Conclusions

In this chapter, we evaluated the gate voltage dependence of the 1/*f* noise of AlGaN/GaN HEMTs for a wide range of temperatures. These results further confirm that the noise is consistent with a number fluctuation model, and not the Hooge mobility fluctuation model that is often applied to AlGaN/GaN HEMTs. The temperature dependence of low frequency noise along with the variations in frequency exponent and gate bias reveals the non-uniformity of the trap distribution in these devices, showing that noise measurements are helpful in understanding the defect-energy distribution in AlGaN/GaN HEMTs.

CHAPTER VI

CONCLUSIONS

In this work, we performed gate voltage dependence of low frequency noise before and after proton irradiation and as a function of temperature of AlGaN/GaN HEMTs built in three different fabrication processes. We find that the Hooge mobility fluctuation model commonly applied to analyze the noise of AlGaN/GaN HEMTs does not correctly identify the origin of the noise in these devices, and often does not describe accurately the frequency, voltage, and/or temperature dependence of these devices. Instead, the noise is described well by a number fluctuation model in which the defect energy distribution of as-processed and irradiated devices varies strongly with energy.

When subjected to 1.8 MeV proton irradiation, a positive threshold voltage shift and degradation in transconductance and ON-current are observed for both the Qorvo and UCSB samples. Acceptor-like traps are created during the irradiation process. Low frequency noise measurements were taken before and after proton irradiation.

We have evaluated in detail the low-frequency noise of AlGaN/GaN HEMTs as a function of proton fluence, voltage, and temperature. Significant deviations were found between the standard mobility fluctuation model expectations and the frequency and gate bias dependence of low frequency noise. We applied the method of Ghibaudo et al. to analyze the low-frequency noise of these devices and found that our results could be well explained by the number fluctuation model with a non-constant defect energy distribution. The first-order estimate of the effective border-trap energy distribution was calculated form the equation modeled by the

number fluctuation model. The non-constant defect energy distribution is reinforced by detailed measurements of temperature dependence of the low frequency noise.

In summary, we have evaluated the radiation response and low frequency noise of AlGaN/GaN HEMTs in detail. Our results indicate the noise is consistent with number fluctuation model with a non-constant defect energy distribution not the previous widely used mobility fluctuation model.

REFERENCES

[1] M. A. Khan, A. Bhattarai, J. N. Kuznia, and D. T. Olson, "High electron mobility transistors based on a GaN/AlGaN heterojunction," *Appl. Phys. Lett.*, vol. 63, no. 9, pp. 1214-1215, Aug. 1993.

[2] U. K. Mishra, P. Parikh, and Y.-F. Wu, "AlGaN/GaN HEMTs-An overview of device operation and application," *Proc. IEEE*, vol. 90, no. 6, pp. 1022-1031, Jun. 2002.

[3] O. Ambacher, J. Majewski, C. Miskys, A. Link, M. Hermann, M. Eickhoff, M. Stutzmann, F. Bernardini, V. Fiorentini, V. Tilak, B. Schaff, and L. F. Eastman, "Pyroelectric properties of Al(In)GaN/GaN hetero- and quantum well structures," *J. Phys.: Condens. Matter*, vol. 14, pp. 3399-3434, 2002.

[4] F. Bernardini and V. Fiorentini, "Nonlinear macroscopic polarization in III-V nitridealloys," *Phys. Rev. B*, vol. 64, no. 8, pp. 085207-1-085207-7, Aug. 2001.

[5] B. Luo, J. W. Johnson, F. Ren, K. K. Allums, C. R. Abernathy, S. J. Pearton, A. M. Dabiran, A. M. Wowchack, C. J. Polley, P. P. Chow, D. Schoenfeld, and A. G. Baca, "Influence of ^{60}Co γ-rays on DC performance of AlGaN/GaN high electron mobility transistors," *Appl. Phys. Lett.*, vol. 80, pp. 604-606, 2002.

[6] O. Aktas, a. Kuliev, V. Kumar, R. Schwindt, S. Toshkov, D. Costescu, J. Stubbins, and I. Adesida, "^{60}Co gamma radiation effects on DC, RF, and pulsed I-V characteristics of AlGaN/GaN HEMTs," *Solid State Electron.*, vol. 48, pp. 471-475, 2004.

[7] A. Ionascut-Nedelcescu, C. Carlone, A. Houdayer, H. J. von Bardeleben, J.-L. Cantin, and S. Raymond, "Radiation hardness of gallium nitride," *IEEE Trans. Nucl. Sci.*, vol. 49, pp. 2733-2738, Dec. 2002.

[8] T. Roy, E.-X. Zhang, Y. S. Puzyrev, D. M. Fleetwood, R. D. Scrimpf, B. K. Choi, A. B. Hmelo, and S. T. Pantelides, "Process dependence of proton-induced degradation in GaN HEMTs," *IEEE Trans. Nucl. Sci.*, vol. 57, no. 6, pp. 3060-3065, Dec. 2010.

[9] T. Roy, E. X. Zhang, Y. S. Puzyrev, X. Shen, D. M. Fleetwood, R. D. Schrimpf, G. Koblmueller, R. Chu, C. Poblenz, N. Fichtenbaum, C. S. Suh, U. K. Mishra, J. S. Speck, and S. T. Pantelides, "Temperature-dependence and microscopic origin of low frequency 1/*f* noise in GaN/AlGaN high electron mobility transistors," *Appl. Phys. Lett.*, vol. 99, no. 20, p. 203501, 2011.

[10] J. Chen, Y. S. Puzyrev, C. X. Zhang, E. X. Zhang, M. W. McCurdy, D. M. Fleetwood, R. D. Schrimpf, S. T. Pantelides, S. W. Kaun, E. C. Kyle, and J. S. Speck, "Proton-induced dehydrogenation of defects in AlGaN/GaN HEMTs," *IEEE Trans. Nucl. Sci.*, vol. 60, no. 6, pp. 4080-4086, Dec. 2013.

[11] J. Chen, Y. S. Puzyrev, R. Jiang, E. X. Zhang, M. W. McCurdy, D. M. Fleetwood, R. D. Schrimpf, S. T. Pantelides, A. R. Arehart, S. A. Ringel, P. Saunier, and C. Lee, "Effects of applied bias and high field stress on the radiation response of AlGaN/GaN HEMTs," *IEEE Trans. Nucl. Sci.,* vol. 62, no. 6, pp. 2423-2430, Dec. 2015.

[12] D. M. Fleetwood and J. H. Scofield, "Evidence that similar defects cause 1/*f* noise and radiation-induced-hole trapping in metal-oxide-semiconductor transistors," *Phys. Rev. Lett.*, vol. 64, pp. 579-582, Jan. 1990.

[13] D. M. Fleetwood, T. L. Meisenheimer, and J. H. Scofield, "1/*f* noise and radiation effects in MOS devices," *IEEE Trans. Electron Dev*., vol. 41, pp. 1953-1964, 1994.

[14] T. L. Meisenheimer and D. M. Fleetwood, "Effect of radiation-induced charge on 1/*f* noise in MOS devices," *IEEE Trans. Nucl. Sci*., vol. 37, pp. 1696-1702, 1990.

[15] D. M. Fleetwood, P. S. Winokur, R. A. Reber, T. L. Meisenheimer, J. R. Schwank, M. R. Shaneyfelt, and L. C. Riewe, "Effects of oxide traps, interface traps, and border traps on metal-oxide-semiconductor devices," *J. Appl. Phys*., vol. 73, pp. 5058-5074, 1993.

[16] D. M. Fleetwood, "1/*f* noise and defects in microelectronic materials and devices," *IEEE Trans. Nucl. Sci*., vol. 62, no. 4, pp. 1462 -1486, Aug. 2015.

[17] M. B. Weissman, "1/*f* noise and other slow, nonexponential kinetics in condensed matter," *Rev. Mod. Phys*., vol. 60, pp. 537-571, 1988.

[18] P. Dutta and P. M. Horn, "Low-frequency fluctuations in solids: 1/*f* noise," *Rev. Mod. Phys*., vol. 53, pp. 497-516, 1981.

[19] M. E. Levinshtein, S. L. Rumantsev, R. Gaska, J. W. Yang, and M. S. Shur, "AlGaN/GaN HEMTs with low 1/*f* noise," *Appl. Phys. Lett*., vol. 73, no. 8, pp. 1089-1091, Aug. 1998.

[20] A. Balandin, "Gate-voltage dependence of low-frequency noise in AlGaN/GaN heterostructure field-effect transistors," *Electron. Lett.*, vol. 36, no. 10, pp. 912-913, 2000.

[21] J. Peransin, P. Vignaud, D. Rigaud, and L. Vandamme, "1/*f* noise in MODFETs at low drain biases," *IEEE Trans. Electron Devices*, vol. 37, no. 10, pp. 2250-2253, 1990.

[22] H. Rao and G. Bosman, "Simultaneous low-frequency noise characterization of gate and drain currents in AlGaN/GaN HEMTs," *J. Appl. Phys.,* vol. 106, no. 10, pp. 103712-1-103712-5, Nov. 2009.

[23] F. Crupi, P. Magnone, S. Strangio, F. Iucolano, and G. Meneghesso, "Low-frequency noise and gate bias instability in normally off AlGaN/GaN HEMTs," *IEEE Trans. Nucl. Sci*., vol. 63, no. 5, pp. 2219-2222, May 2016.

[24] S. Vodapally, C. H. Won, I. T. Cho, J. H. Lee, Y. Bae, S. Cristoloveanu, K. S. Im, and J. H. Lee, "1/*f* noise characteristics of AlGaN/GaN omega shaped nano-wire FETs," *Proc. EuroSOI ULIS.*, pp. 44-47, Jan. 2016.

[25] A. L. McWhorter, "1/*f* noise and germanium surface properties," in Semiconductor Surface Physics, PA, Philadelphia:Univ. Pennsylvania Press, pp. 207-228, 1957.

[26] F. N. Hooge, T. G. M. Kleinpenning, and L. K. J. Vandamme, "Experimental studies on 1/*f* noise," *Rep. Prog. Phys.,* vol. 44, no. 5, pp. 479-532, 1981.

[27] A. A. Balandin, Noise and Fluctuation Control in Electronic Devices, CA, Los Angeles:Amer. Sci. Publishers, 2002.

[28] H. D. Hao, "Low frequency noise and charge trapping in MOSFETs," PhD diss., *Vanderbilt University*, 2004.

[29] M. J. Kirton and M. J. Uren, "Noise in solid-state microstructures-a new perspective on individual defects, interface states and low-frequency (1/*f*) noise," *Adv. Phys.*, vol. 38, pp. 367-468, 1989.

[30] K. S. Ralls, W. J. Skocpol, L. D. Jackel, R. E. Howard, L. A. Fetter, R.W. Epworth, and D. M. Tennant, "Discrete resistance switching in submicrometer Si inversion layers: Individual interface traps and low frequency (1/*f*) noise," *Phys. Rev. Lett*., vol. 52, pp. 228-231, Jan. 1984.

[31] S. Christenson, I. Lundstrom, and C. Svennson, "Low-frequency noise in MOS transistors-theory," *Solid-State Electron.*, vol. 11, pp. 797-812, 1968.

[32] H. Mikoshiba, "1/*f* noise in n-channel Si gate MOS transistors," *IEEE Trans. Electron Devices*, vol. 29, no. 6, pp. 965-970, Jun. 1982.

[33] J. H. Scofield and D. M. Fleetwood, "Physical basis for nondestructive tests of MOS radiation hardness," *IEEE Trans. Nucl. Sci.,* vol. 38, no. 6, pp. 1567-1577, Dec. 1991.

[34] F. N. Hooge, "1/*f* noise is no surface effect," *Phys. Lett*., vol. 29A, pp. 139-140, 1969.

[35] L. K. J. Vandamme and X. S. Li, D. Rigaud, "1/*f* noise in MOS devices: Mobility or number fluctuations?" *IEEE Trans. Electron Devices*, vol. 41, no. 11, pp. 1936-1945, Nov. 1994.

[36] G. Ghibaudo, O. Roux, Ch. Nguen-Duc, F. Balestra, and J. Brini, "Improved analysis of low frequency noise in field-effect MOS transistors," *Phys. Stat. Sol. A*., vol. 124, pp. 571-581, 1991.

[37] D. M. Fleetwood, P. Wang, J. Chen, R. Jiang, E. X. Zhang, M. W. McCurdy, and R. D. Schrimpf, "1/*f* noise in GaN/AlGaN HEMTs," *Proc. Intl. Conf. Solid-State Integ. Circ. Technol*., Oct. 25-28, Hangzhou, China, paper no. S03-02.

[38] P. Wang, R. Jiang, J. Chen, E. X. Zhang, M. W. McCurdy, R. D. Schrimpf, and D. M. Fleetwood, "1/*f* noise in as-processed and proton-irradiated AlGaN/GaN HEMTs due to carrier number fluctuations," *IEEE Trans. Nucl. Sci*., vol. 64, no. 1, pp. 181-189, 2017.

[39] C. Della-Morrow, C. Lee, K. Salzman, R. Coffie, V. Li, G. Drandova, T. Nagle, D. Morgan, P. Horng, S. Hillyard, and J. Ruan, "Achieve manufacturing readiness level 8 of high-power, high efficiency 0.25 μm GaN on SiC HEMT Process," *presented at the CS MANTECH Conf*., New Orleans, LA, USA, May 13-16, 2013.

[40] G. I. Drandova, J. L. Jimenez, P. T. Goeller, and A. P. Ferreira, "TriQuint's 2nd generation TQGaN25 technology reliability assessment," *Proc. JEDEC Workshop on Reliability of Compound Semiconductors*, pp. 95-97, 2013.

[41] N. E. Ives, J. Chen, A. F. Witulski, R. D. Schrimpf, D. M. Fleetwood, R. W. Bruce, M. W. McCurdy, E. X. Zhang, and L. W. Massengill, "Effects of proton-induced displacement damage on GaN HEMTs in RF power amplifier applications," *IEEE Trans. Nucl. Sci*., vol. 62, no. 6, pp. 2417-2422, 2015.

[42] S. W. Kaun, M. H. Wong, J. Lu, U. K. Mishra, and J. S. Speck. "Reduction of carbon proximity effects by including AlGaN back barriers in HEMTs on free-standing GaN," *Electron. Lett*. vol. 49, pp. 893-895, Jul. 2013.

[43] R. Jiang, E. X. Zhang, M. W. McCurdy, J. Chen, X. Shen, P. Wang, D. M. Fleetwood, R. D. Schrimpf, S. W. Kaun, E. C. H. Kyle, J. S. Speck, and S. T. Pantelides, "Worst-case bias for irradiation of AlGaN/GaN HEMTs," *IEEE Trans. Nucl. Sci*., vol. 64, no. 1, pp. 218-225, Jan. 2017.

[44] B. Luo, J. W. Johnson, F. Ren, K. K. Allums, C. R. Abernathy, S. J. Pearton, R. Dwivedi, T. N. Fogarty, R. Willams, A. M. Dabiran, A. M. Wowchack, C. J. Polley, P. P. Chow, and A. G. Baca, "DC and RF performance of proton-irradiated AlGaN/GaN high electron mobility transistors," *Appl. Phys. Lett.*, vol. 79, pp. 2196-2199, Feb. 2001.

[45] B. D. White, M. Bataiev, L. J. Brillson, B. K. Choi, D. M. Fleetwood, R. D. Schrimpf, S. T.Panelides, R. W. Dettmer, W. J. Schaff, J. G. Champlain, and U. K. Mishra, "Characterization of 1.8 MeV proton irradiated AlGaN/GaN field-effect transistor structures by nanoscale depth-resolved luminescence spectroscopy," *IEEE Trans. Nucl. Sci*., vol. 49, no. 6, pp. 2695-2701, Dec. 2002.

[46] X. Hu, A. Karmarkar, B. Jun, D. M. Fleetwood, R. D. Schrimpf, R. D. Geil, R. A. Weller, B. D. White, M. Bataiev, L. J. Brillson, and U. K. Mishra, "Proton-irradiation effects on AlGaN/AlN/GaN high electron mobility transistors," *IEEE Trans. Nucl. Sci*., vol. 50, no. 6, pp. 1791-1796, 2003.

[47] A. Kalavagunta, A. Touboul, L. Shen, R. D. Schrimpf, R. A. Reed, D. M. Fleetwood, R. K. Jain, and U. K. Mishra, "Electrostatic mechanisms responsible for device degradation in proton irradiated AlGaN/AlN/GaN HEMTs," *IEEE Trans. Nucl. Sci*., vol. 55, no. 4, pp. 2106-2112, Aug. 2008.

[48] S. J. Pearton, F. Ren, E. J. Patrick, M. E. Law, and A. Y. Polyakov, "Review-Ionizing radiation effects on GaN devices," *ECS Journal of Solid State Science and Technology*, vol. 5, no. 2, pp. Q35-Q60, 2016.

[49] S. A. Francis, A. Dasgupta, and D. M. Fleetwood, "Effects of total dose irradiation on the gate-voltage dependence of the 1/*f* noise of nMOS and pMOS transistors," *IEEE Trans. Electron Devices,* vol. 57, no. 2, pp. 503-510, Feb. 2010.

[50] C. Surya and T. Y. Hsiang, "A thermal activation model for $1/f^{\gamma}$ noise in Si-MOSFETs," *Solid State Electron*., vol. 31, no. 5, pp. 959–964, May 1988.

[51] H. Wong and C. Cheng, "Study of electronic trap distribution at the SiO_2-Si interface utilizing the low-frequency noise measurement," *IEEE Trans. Electron Devices*, vol. 37, no. 7, pp. 1743-1749, Jul. 1990.

[52] J. I. Lee, J. Brini, A. Chovet, and C. A. Dimitriadis, "On $1/f^{\gamma}$ noise in semiconductor devices", *Solid State Electron.*, vol. 43, no. 12, pp. 2181-2183, Dec. 1999.

[53] D. M. Fleetwood, T. L. Meisenheimer, and J. H. Scofield, "1/*f* noise and radiation effects in MOS devices," *IEEE Trans. Electron Devices*, vol. 41, no. 11, pp. 1953-1964, 1994.

[54] C. X. Zhang, E. X. Zhang, D. M. Fleetwood, R. D. Schrimpf, S. Dhar, S.-H. Ryu, X. Shen, and S. T. Pantelides, "Origins of low-frequency noise and interface traps in 4H-SiC MOSFETs," *IEEE Electron Device Lett*., vol. 34, no. 1, pp. 117-119, Jan. 2013.

[55] M. Silvestri, M. J. Uren, N. Killat, D. Marcon, and M. Kuball, "Localization of off-stress-induced damage in AlGaN/GaN HEMTs by means of low-frequency 1/*f* noise measurements," *Appl. Phys. Lett*., vol. 103, no. 4, p. 043506, 2013.

[56] G. Ghibaudo, "Calculation of surface charge noise at the Si-SiO_2 interface," *Phys. Stat. Sol.(a)*, vol. 124, pp. 571-581, 1991.

[57] D. Wang, C. Wu, and C. Wu, "Determination of polarization charge density on interface of AlGaN/GaN heterostructure by electroreflectance," *Appl. Phys. Lett*., vol. 89, no. 16, p.161903, 2001.

[58] Z. Celik-Butler and T. Y. Hsiang, "Spectral dependence of 1/*f*$^{\gamma}$ noise on gate bias in N-MOSFETS," *Solid-State Electron.*, vol. 30, pp. 419-423, 1987.

[59] T. Roy, Y. S. Puzyrev, E. X. Zhang, S. DasGupta, S. A. Francis, D. M. Fleetwood, R. D. Schrimpf, U. K. Mishra, J. S. Speck, and S. T. Pantelides, "1/*f* noise in GaN HEMTs grown under Ga-rich, N-rich, and NH_3-rich conditions," *Microelectron. Reliab*., vol. 51, pp. 212-216, 2011.

[60] Y. Puzyrev, T. Roy, E. X. Zhang, D. M. Fleetwood, R. D. Schrimpf, and S. T. Pantelides, "Radiation-induced defect evolution and electrical degradation of AlGaN/GaN HEMTs," *IEEE Trans. Nucl. Sci*., vol. 58, no. 6, pp. 2918-2924, Dec. 2011.